ESTIMATING CANOPY FUEL PARAMETERS WITH IN-SITU AND REMOTE SENSING DATA

A Dissertation

by

MUGE MUTLU

Submitted to the Office of Graduate Studies of
Texas A&M University
in partial fulfillment of the requirements for the degree of

DOCTOR OF PHILOSOPHY

December 2010

Major Subject: Forestry

Estimating Canopy Fuel Parameters with In-Situ and Remote

Sensing Data

ESTIMATING CANOPY FUEL PARAMETERS WITH IN-SITU AND REMOTE SENSING DATA

A Dissertation

by

MUGE MUTLU

Submitted to the Office of Graduate Studies of
Texas A&M University
in partial fulfillment of the requirements for the degree of

DOCTOR OF PHILOSOPHY

Approved by:

Chair of Committee,	Sorin C. Popescu
Committee Members,	Ross F. Nelson
	X. Ben Wu
	Anthony M. Filippi
	Marian Eriksson
Head of Department,	Steven G. Whisenant

December 2010

Major Subject: Forestry

ABSTRACT

Estimating Canopy Fuel Parameters with In-Situ and Remote Sensing Data. (December 2010)

Muge Mutlu, B.A., Cukurova University, Turkey;

M.S., Texas A&M University

Chair of Advisory Committee: Dr. Sorin C. Popescu

Crown fires, the fastest spreading of all forest fires, can occur in any forest type throughout the United States and the world. The occurrence of crown fires has become increasingly frequent and severe in recent years. The overall aim of this study is to estimate the forest canopy fuel parameters including crown base height (CBH) and crown bulk density (CBD), and to investigate the potential of using airborne lidar data in east Texas. The specific objectives are to: (1) propose allometric estimators of CBD and CBH and compare the results of using those estimators to those produced by the CrownMass/FMAPlus software at tree and stand levels for 50 loblolly pine plots in eastern Texas, (2) develop a methodology for using airborne light detection and ranging (lidar) to estimate CBD and CBH canopy fuel parameters and to simulate fire behavior using estimated forest canopy parameters as FARSITE inputs, and (3) investigate the use of spaceborne ICEsat /GLAS (Ice, Cloud, and Land Elevation Satellite/Geoscience Laser Altimeter System) lidar for estimating canopy fuel parameters. According to our results from the first study, the calculated average CBD values, across all 50 plots, were 0.18

kg/m³ and 0.07 kg/m³, respectively, for the allometric equation proposed herein and the CrownMass program. Lorey's mean height approach was used in this study to calculate CBH at plot level. The average height values of CBH obtained from Lorey's height approach was 10.6 m and from the CrownMass program was 9.1 m. The results obtained for the two methods are relatively close to each other; with the estimate of CBH being 1.16 times larger than the CrownMass value. According to the results from the second study, the CBD and CBH were successfully predicted using airborne lidar data with R^2 values of 0.748 and 0.976, respectively. The third study demonstrated that canopy fuel parameters can be successfully estimated using GLAS waveform data; an R^2 value of 0.84 was obtained. With these approaches, we are providing practical methods for quantifying these parameters and making them directly available to fire managers. The accuracy of these parameters is very important for realistic predictions of wildfire initiation and growth.

DEDICATION

To my son, Arda Kaan Mutlu

ACKNOWLEDGEMENTS

First, thanks to God for everything that I have today.

I would like to express my sincere appreciation to Dr. Sorin C. Popescu, my committee chair and advisor, for giving me the opportunity to pursue my PhD degree. I would not have been successful without his help. He provided the constant encouragement, advice, and motivation that I really needed in order to get this work done. His performance and original thoughts have pushed me to learn and grow more and more.

I wish to thank all my committee including: Dr. Nelson, Dr. Eriksson, Dr. Wu, and Dr. Filippi for all their advice, support, and patience. Thanks also go to my friends and colleagues for their help, encouragement, and understanding. Especially, I would like to thank my real friends, Kaiguang Zhao (Dr. K) and Pushpa Tuppad. I would not have done this without their motivation, help, and advice.

I express my gratitude to the Spatial Science Lab, Department of Ecosystem Science and Management, and Texas A&M University for providing me with the assistance and invaluable resources to complete this degree.

Thanks to my mother, Sevinc Agca, and father, Tahsin Agca, for their encouragement, support, and love.

Finally, the biggest and warmest thanks go to my 4 year old son Arda Kaan. You are my world and life. Thanks for being so good when I had to study. You are a great boy and I love you so much.

TABLE OF CONTENTS

CHAPTER Page

LIST OF FIGURES

Page

LIST OF TABLES

CHAPTER I

INTRODUCTION

The occurrence of wildland fires is an essential part of the natural cycle of the ecosystem (Johnson, 1992). Without fire, ecosystems may turn into a major disturbance mechanism (Pyne et al., 1996). A fire clears out a great deal of vegetation, leaving behind burned and/or partially burned areas. On the surface this can appear to be a loss, but it actually provides a new habitat for young and different plants to grow (Omi, 2005; Pyne et al., 1996). Over time, certain fire adapted species and fire dependent relationships develop. A fire dependent species is one that has adapted to fire so much that it requires fire to complete an essential part of its life cycle. In some species such as *Picea mariana*, *E. regnans, E. diversicolor,* and *P. banksiana*, seeds are stored in tree crown, called serotiny (Lamont et al., 1991). Fires actually help these seeds by releasing them into recruitment environment and dropping their seeds and reduce the competition. If fires do not recur frequently enough, some species may disappear (Pyne, et al., 1996).

Wildland fires, though an integral part of nature, can also create a societal problem. They affect forest structures in different ways such as altering vegetation composition, increasing soil erosion, heating stream water, modifying the hydrological cycle, and endangering human lives and properties in large areas of wildland/urban interface (Agee & Skinner, 2005; Chuvieco, 1999). All fire behavior properties are strongly related to fuel characteristics, weather, and topography information for instance

---

This dissertation follows the style of *Remote Sensing of Environment.*

digital elevation model, slope, and aspect (Mutlu et al., 2008b). Fire behavior is used to describe the reaction of the fire to fuel, topography, weather, direction, and the pattern of fire spread (DeBano et al., 1998). Vegetation types can be grouped into fuel types based on similar potential fire behavior (Riano et al., 2002). Since forest structure is related to fire behavior, fire risk and behavior depends on the quantity of biomass, the vertical and horizontal structure of the canopy, and live and dead biomass portion.

Fuel distribution is a critical factor for predicting fire behavior. Fuel is any living or dead organic combustible material including grass, leaves, ground litter, and shrubs and trees that can ignite and burn. A fuel type is an identifiable organization of fuel elements of plant species, form, size, arrangement, or other fuel elements that will cause a predictable rate of fire spread (Pyne et al., 1996). Forest fuels are classified as ground, surface, and crown fuels. Ground fuels are defined as all burnable materials below the surface litter such as organic soils, duff, tree or shrub roots, rotten buried logs, peat, and sawdust, which usually support a glowing combustion without flame (Scott & Reinhardt, 2001). Ground fuels are characterized by higher bulk density than surface and canopy fuels. Surface fuels are described as surface litter on the soil surface. This includes needles, leaves, grass, twigs, bark, cones, dead and down branch wood and logs, shrubs, low brush, and short trees available to burn. Crown fuels, also called aerial, are described as all burnable materials, e.g., live and dead foliage, lichen, live and dead brachwood, that are located in the upper forest canopy and separated from the ground by more than six feet (Chuvieco & Congalton, 1989). They have higher moisture content and lower bulk density than surface fuels. When fuels are arranged uniformly and

continuously, fire will travel uniformly, but canopy structure is highly heterogeneous and causes fires to spread along combustible paths (Pyne et al., 1996; Riano et al., 2002).

The accurate prediction of the potential risk of a wildland fire can help reduce the seriousness of wildland fires. There are three general types of wildland fires recognized by fire scientists and managers. A ground fire burns in ground fuels, underneath the surface litter of the forest floor. Ground fires spread within the organic layer and are characterized by a slowly smoldering edge with no flame and very little smoke because of the compactness of ground fuels. These types of fires are difficult to detect and control (DeBano et al., 1998). Ground fires may follow surface fires that may cause much of the initial spread. A surface fire occurs in the surface fuel layer and surface fire behavior varies widely depending on the nature of the surface fuel complex. A surface fire may turn into the crown fire depending on the surface fuels and crown characteristics. Crown fires result, when surface fires have created enough energy to preheat and combust live crown fuels (Agee & Skinner, 2005). Crown fires advance from top to top of trees or shrubs and spread through the overstory (Pyne et al., 1996; Cohen et al., 2006) They are the fastest spreading of all forest fires, more difficult to control, and their effects are more lasting than surface fires (Rothermel, 1983). Decision-making tools for canopy fuel management practices are based on the relationships between crown fire behavior, surface fire behavior, and canopy fuel structure. Recent advances in lidar technology and applications research have demonstrated the ability of lidar data to accurately map crown fuels in test areas (Hyyppa et al., 2000; Riano et al., 2004; Andersen et al., 2005; Hyde et al., 2005).

Forest managers must consider the vertical distribution of fuels when evaluating the potential risk associated with a crown fire. According to Van Wagner (1977) there are three types of crown fires: passive, active, and independent. A passive crown fire, also known as a torching fire, occurs when the surface flame spreads to the canopy and flaming in the canopy can be maintained only for short periods (Scott & Reinhardt, 2001; Van Wagner, 1977). Active crown fires, known as continuous crown fires, spread by torching and are continual based on the density of the forest canopy fuels. This type of fire depends on heat from the surface fuels for constant spread (Agee & Skinner, 2005). An independent crown fire is one that continues to burn in canopy fuels without requiring heat from surface fire; but it requires steep slope, strong windspeed, and low moisture (Scott & Reinhardt, 2001).

There is a strong interest in the use of recent advances in high spectral resolution remotely sensed imagery in forest fuel inventories. Applications of various remote sensing systems and techniques to forest fire related research have been rapidly increasing in recent years. These techniques and systems can be used to decrease fire risk and reduce fire damage (Mutlu et al., 2008a; Andersen et al., 2005; Arroyo et al., 2008; Mutlu et al., 2008b). A number of studies have used multispectral remote sensing data to map fuels (Wulf et al., 1990; Salas & Chuvieco, 1995; Castro & Chuvieco, 1998; Maselli et al., 2000; Mutlu et al., 2008a). However, there are limitations in using these optical images (i.e. Landsat, SPOT, QuickBird, IKONOS, etc.) including their inability to penetrate forest canopies (Keane et al., 2000; Arroyo et al., 2008) and to detect surface fuels when more than two canopies are present. Also, reflectance from the

surface is not related to vegetation height. Lidar pulses can penetrate into a canopy and can be used to infer the height fuel elements.

Airborne lidar remote sensing is an advanced technology for forestry applications. It provides useful information about the three-dimensional structure of forests, which makes it a valuable tool for the mapping of wildland fires (Means et al., 2000). Lidar sensors are active remote sensing tools that measure properties of scattered light to find range and/or other information about an object (Popescu et al., 2004). Airborne lidar directly measures the three-dimensional distribution of tree canopies and allows accurate and efficient estimation of canopy fuel characteristics over large areas of forests (Andersen et al., 2005; Nelson et al., 2003; Popescu et al., 2002). In recent years, lidar remote sensing techniques have been applied to estimate surface fuel models and canopy fuel parameters (Mutlu et al., 2008a; Arroyo et al., 2008; Dubayah & Drake, 2000; Riano et al., 2003; Andersen et al., 2005; Hall et al., 2005; Morsdorf et al., 2004; Popescu & Zhao, 2008). The Geoscience Laser Altimeter System (GLAS) on the Ice, Cloud and land Elevation satellite (ICESat) is the first spaceborne lidar tool. This system was designed to measure and monitor ice sheet mass balance, cloud and aerosol heights, surface elevation changes, and vegetation characteristics (Zwally et al., 2002; Sun et al., 2008; Nelson et al., 2009; Simard et al., 2008). The ICESat/GLAS has become more popular and used in various forest studies such as deriving forest characteristics, forest biomass estimation, and forest structure analysis (Drake et al., 2002; Popescu, 2007). Spaceborne lidar waveform data were used to obtain digital elevation information (DEM), and canopy base height (CBH).

Objectives

This study has three main objectives:

(1) provide canopy bulk density (CBD) and canopy base height (CBH) estimators for a loblolly pine dominated area in Huntsville, TX, at the plot level using both allometric equations and the CrownMass/FMAPlus software,

(2) develop a methodology for assessing and mapping CBD and CBH with lidar derived metrics at multiple spatial resolutions for loblolly pine dominated areas, and

(3) investigate the use of spaceborne ICEsat /GLAS lidar data for characterizing forest canopy fuel parameters in eastern Texas.

Dissertation Organization

The dissertation consists of six chapters. An introduction to the dissertation is presented here in Chapter I. Chapter II contains a literature review. Chapter III presents a methodology for estimating CBD and CBH specifically for loblolly pine dominated areas plot level using both allometric equations and CrownMass/FMAPlus software. Chapter IV presents a methodology for estimating CBH and CBD using airborne lidar data for loblolly pine trees in eastern Texas and simulation results of FARSITE. Chapter V presents a methodology for investigating the use of spaceborne ICEsat /GLAS lidar data to derive CBH. Conclusions of the study are presented in Chapter VI. In this dissertation, chapters III, IV, and V are organized as individual manuscripts.

CHAPTER II

LITERATURE REVIEW

Previous studies have shown that airborne lidar remote sensing technology can be used to estimate a variety of forest inventory parameters, including aboveground biomass, stem volume, stand height, basal area, mean diameter at breast height (dbh), stem density, canopy bulk density (CBD), canopy cover, and canopy base height (CBH) (Means et al., 2000; Lefsky et al., 2002; Maclean & Krabill, 1986; Means et al., 1999; Nelson et al., 1984; Popescu, 2007). Some studies have also shown the ability to transform lidar measurements to approximate canopy height and the vertical distributions of foliage density (Carreiras et al., 2006; Means et al., 1999). Estimates of CBD and CBH are necessary spatial data inputs for fire simulation software such as FARSITE (Finney, 1995). These two canopy fuel parameters have been estimated by many researchers through allometric equations and/or remote sensing technology.

A lidar study in Norway developed an approach to estimate Lorey's mean height, crown lengths, and heights to crown base for plots in a spruce-pine forest using height quantile estimators (Naesset & Okland, 2002). The average space of laser pulses was ranged from 0.66 m to 1.29 m. The canopy metrics obtained from the laser pulses were used in their regression analysis using ground truth values. Riano et al. (2004) study presented a methodology for estimating crown fuel parameters at individual tree and plot levels in an intensively managed, homogeneous Scots pine forest with little understory. They used the equations developed in the Riano et al. (2003) to derive these two canopy

fuel parameters. Then, they assessed the ability of using lidar data to estimate CBD and CBH. Andersen et al. (2005) presented and evaluated an approach for estimating critical canopy fuel metrics; including canopy fuel weight, CBD, CBH, and canopy height, using high density, multiple-return lidar data collected over a Pacific Northwest conifer forest. A cross-validation procedure was used to assess the reliability of these models. They used the Fire and Fuels Extension to the Forest Vegetation Simulator (FFE-FVS) method to estimate canopy fuel parameters. Falkowski et al. (2005) evaluated the accuracy and utility of imagery from the Advanced Spaceborne Thermal Emission and Reflection (ASTER) radiometer satellite sensor and gradient modeling for mapping fuel layers for fire behavior modeling with FARSITE and FlamMap. They created the surface fuels map using a classification tree based on three gradient layers: cover type, potential vegetation type, and structural stage. Single band reflectance values (green, red, and near-infrared (NIR)) and vegetation indices (NDVI, GRVI and SR) were used as predictor variables in their regression analysis. Model coefficients were extracted from the best model for each response variable and used to create the final crown closure and crown bulk density layers.

Lefsky et al. (2005) focused on statistical relationships between two multivariate datasets containing lidar measurements of canopy structure and field measurements of stand structure. They transformed SLICER waveforms into four canopy structure classes to analyze the relationship between the canopy and stand structure. Then, Canonical Correlation Analysis was used to create correlated axes pairs from the canopy and stand structure. Each pair of axes was examined using their correlations with the original stand

and canopy indices. In a study by Popescu and Zhao (2008), airborne lidar data were used to assess CBH for individual trees in east Texas. They used TreeVaw, a lidar software application developed by Popescu et al. (2003), to position individual trees and to obtain each tree's height and crown width measurements. By using linear regression models, they were able to explain approximately 80% of the variability related with individual trees' canopy base height. Taylor et al. (1998) assessed temporal changes in crown fire hazard at the landscape scale by noting the change in relative frequency of different types of crown fire in different time periods. Skowronski et al. (2007) measured canopy height using the first return profiling lidar portable airborne laser system (PALS), obtained intensive biometric measurements in plots, and used Forest Inventory and Analysis (FIA) data to characterize forest structure and ladder fuels in the New Jersey Pinelands, USA. Height percentiles at different height intervals above the ground were predicted from the airborne lidar datasets. The arithmetic and quadratic mean of both all first lidar returns and all first returns from the canopy (>3 m and >4 m) were analyzed to detect the presence/absence of ladder fuels using a profiling lidar. They estimated understory cover in different height classes (1-4 m) and generated a fuel loading map for their area. They concluded that different lidar height classes generated in their study can be used to detect ladder fuels and to evaluate fuel reduction treatments. Jia et al. (2006) focused on estimating forest canopy cover, separating ponderosa pine and Douglas-fir, and assessing the burn severity of two recent fires using remote sensing data.

In a study by Naesset and Gobakken (2008), airborne lidar data was used to estimate above and below ground biomass in young and mature coniferous forest in Norway. Canopy height and density were estimated and used as independent variables in their regression analysis. They used four different airborne lidar data sets obtained from four different laser scanners to obtain all forest parameters necessary to predict biomass in their study. Height percentiles, mean and maximum height values, coefficients of variation in heights, and canopy density at different height intervals above the ground were also predicted from the four different airborne lidar datasets.

In recent years, ICESat/GLAS has been used in a number of forestry studies. GLAS data has proven to have strong correlation with field-based aboveground biomass and canopy height measurements in extensive forests (Boudreau et al., 2008; Sun et al., 2008). Lefsky et al. (2005) used ICESat/GLAS data to estimate maximum stand height and aboveground biomass in three forested ecosystems located in Brazil, and two states in the USA, Tennessee and Oregon. Ranson et al. (2004) used GLAS waveform data to identify and examine forest disturbance, fire, and forest stands damaged by insects in central Siberia. They compared GLAS waveforms for damaged and undamaged forest stands and found that crown structure information can be derived from GLAS data. Duong et al. (2006) used ICESat/GLAS waveform data for land cover classification in the Netherlands. Nelson et al. (2009) used GLAS waveform and MODerate resolution Imaging Spectrometer (MODIS) data to assess Siberian timber volume in south-central Siberia. They attributed a MODIS land cover map with timber volume estimates obtained from GLAS data, and then compared the timber volume estimates to ground

based estimates in their area. Based on their results, the GLAS/MODIS estimate was 77.38×109 m3, a difference of less than 1.1%.

Some studies used a nominal elliptical shape of GLAS footprint. Popescu et al. (in review) compared estimated total aboveground biomass and canopy height metrics derived from both GLAS waveform and airborne lidar data. Instead of using circular shape, they used an elliptical shape of GLAS footprints to extract height metrics and biomass estimates from airborne lidar data in their study. Their results demonstrate that GLAS waveform data can be used to accurately assess aboveground biomass in eastern Texas. Pang et al. (2008) and Neuenschwander et al. (2008) estimate stand height metrics from both GLAS waveforms and airborne lidar data also using the nominal shape of GLAS footprints and then compared the results. Sun et al. (2008) used GLAS data along with LVIS data (Laser Vegetation Imaging Sensor) to model vertical structure of characteristics of the forests in Maryland, USA. Based on their results, GLAS waveform data can be used to estimate vertical structure of the stand. Simard et al. (2008) focused on how to use ICESat/GLAS to estimate the extent, height, and biomass of the mangrove forests in Colombia using SRTM (Shuttle Radar Topography Mission) elevation data, ICEsat/GLAS waveforms, and field data. In a study by Boudreau et al. (2008), the combination of ICESat/GLAS waveform data and airborne lidar data was used to predict regional aboveground dry biomass in forests in Quebec at a very large spatial scale. They compared their aboveground biomass estimates with those obtained from other biomass estimations that are available from previous studies and found a high correlation.

Airborne lidar data have also been used for mapping the spatial distribution of forest surface fuels, and canopy fuel parameters (Mutlu et al., 2008a; Popescu & Zhao, 2008). Such maps are required inputs for fire simulation software such as FlamMap, FARSITE, and NEXUS. Fire managers around the world use FARSITE software (Finney, 1994; Keane et al., 1998). There are few published studies that use fire behavior models to evaluate potential fire behavior in a given landscape (Finney, 1995; Stephens, 1997; Faiella, 2005; Stratton, 2004). Stephens (1997) used FARSITE to spatially simulate fire growth and behavior in a mixed-conifer forest in California and to investigate silvicultural and fuel treatments affect on potential fire behavior in that forest. Mutlu et al. (2008a) fused lidar and multispectral Quickbird data to produce surface fuel model maps, one of the key inputs in FARSITE. Mutlu et al. (2008b) used these results to create two different datasets, one obtained from lidar data alone and the other one obtained from different sources. These datasets were used as inputs into FARSITE. Keane et al. (2000) combined both gradient modeling and remote sensing to map fuels spatial data layer required by FARSITE to spatially model fire behavior on the Gila National Forest, New Mexico. Miller and Yool (2002) evaluated the sensitivity of FARSITE to the level of detail in the fuels data, both spatially and quantitatively, which provided land managers knowledge about the effectiveness of detailed fuels mapping in modeling fire spread. In their study, two surface fuel maps were generated using two different scales, fine and coarse. They ran FARSITE and found that fine scale fuel maps produce statistically smaller fire areas.

Several researchers (Stephens, 1997; Agee et al., 2000; Fule et al., 2001) assessed fire hazard and the effectiveness of fuel treatments on crown fire potential. Scott and Reinhardt (2001) focused on assessing surface and crown fire behavior models and transitioned between them using Van Wagner's crown fire transition criteria in a forest stand. Russel and McBride (2003) sampled various vegetation types throughout seven sites using a chronosequence of remote sensing images in order to detect change over time. They also estimated changes in fuel and fire hazard through field sampling and by using the FARSITE software. They assessed the average rate of spread, flame length, and fire-line intensity for each of the vegetation types in their study area.

Mbow et al. (2004) described the use of spectral indices and simulation of savanna burning to assess the risk of intensive fire propagation in a national park in West Africa. They developed a simple remote sensing based algorithm to detect fire risk areas and their corresponding risk levels. In their study, the FARSITE fire simulation software was used to address the fire risk assessment issue in their area. Mitsopoulos and Dimitrakopoulos (2007) derived canopy fuels for Aleppo pine stands and simulated crown fire behavior using different understory fuel types in Greece. Stratton (2004) presented a methodology for assessing the effectiveness of landscape fuel treatments on fire growth and behavior in southern Utah. He used FARSITE and FlamMap to model pre- and post-treatment effects on fire growth, spotting, and fireline intensity.

Some studies estimated crown foliage and branch biomass at tree-level using allometric equations (e.g. Brown 1978; Riano et al., 2003; Fule et al., 2004). Roccaforte et al. (2008) estimated canopy fuel parameters (CBH and CBD) and analyzed stand

characteristics for the untreated, densely treated areas, and treated stands in the Mount Trumbull, Arizona, USA forest to evaluate fire risk and the effectiveness of fuel treatments on crown fire. The CBD values were computed as the available canopy fuel load divided by canopy volume using equations from Fule et al. (2001), Brown (1978), and Cruz et al. (2003). The CBH values were calculated using regression equations for ponderosa pine trees in Grand Canyon, Arizona, USA. Then, they used their estimates of CBD and CBH as inputs into FlamMap and NEXUS fire behavior and hazard assessment systems to estimate and compare results of potential fire behavior. Several species-specific studies predict foliar and branch biomass from tree dimensions.

Brown (1978) developed predictive equations for ponderosa pine stands in the northern Rocky Mountains. His results have been widely applied to estimate canopy fuel weight and density (Keane et al., 2000; Pollet & Omi 2002; Raccoforte et al., 2008). Snell and Brown (1980) provide similar algorithms for Pacific Northwest conifers. Whittaker and Woodwell (1968) studied the distribution of biomass within individual pine trees. Foresters and ecologists commonly use their study**.** Using data from the USDA Forest Service's Forest Inventory and Analysis (FIA) database, Cruz et al. (2003) developed equations for crown fuel load (CFL), CBD, and CBH, for different vegetation types in the western U.S. The crown fire spread rate was modeled using non-linear regression analysis in their study.

Baldwin and Peterson (1997) developed a model to predict the crown shape of loblolly pine trees in stands and developed species-specific equations for loblolly pine trees in Louisiana, USA. Their system of equations includes models for the crown

height, volume, surface area, and maximum crown radius. Hall and Burke's (2006) study focused on analyzing the effects and sensitivity of assumptions made for CBH and CBD using data from the Colorado Front Range, USA. They also focused on the role of crown shape information in the calculations of CBD and CBH and found that these two variables are very sensitive to crown shape. Fahnestock (1970) developed a heuristic key to crowning potential rate based largely on canopy closure, crown density, and the presence or absence of ladder fuels at tree level. Kilgore and Sando (1975) showed a decrease in crown fire potential following prescribed burning in a giant sequoia/mixed-conifer forest by comparing canopy fuel weight, crown volume ratio, mean height to canopy base, and the vertical profile of canopy fuel packing ratio before and after a prescribed fire.

This current study builds on and extends the research efforts described above by integrating airborne lidar and space borne IceSat/GLAS data to estimate canopy fuel parameters using wall-to-wall lidar-derived CBD and CBH maps. Species-specific equations for foliage biomass and crown volume are rarely developed and used to predict CBD. We employed a unique approach to model CBD and CBH for loblolly pine stands in eastern Texas and compared estimates obtained from those models to those of CrownMass, a program often used to predict canopy fuel parameters. The results of these two methods were used as ground reference data when estimating both CBD and CBH from airborne lidar data. Our study is unique because it is the first study that models CBH from ICESat/GLAS waveform data using a wall-to-wall canopy fuel map obtained from airborne lidar data. In addition, we developed all of the spatial data

layers required by FARSITE including, fuel model map, canopy cover, DEM, slope, aspect, CBD, canopy height model (CHM), and CBH using airborne lidar data and simulated crown fire behavior in eastern Texas. Many fire managers do not have a surface fuel model map, CBD, and CBH data layers and as far as I am aware, there is no published study that runs FARSITE to simulate crown fires in Texas.

CHAPTER III

ESTIMATING CANOPY FUEL PARAMETERS FOR LOBLLOLY PINE TREES USING FIELD DATA

Introduction

In recent years, the number of crown fires has significantly increased, threatening life, property, and natural resources in the United States (Falkowski et al., 2005). Wildland crown fires are one of the most important and prevalent type of disasters because of their potential environmental impacts (Pyne et al., 1996). Fire managers and foresters use the term "crown" to refer to the branches and foliage of individual trees, and the term "canopy" refers to the aggregation of crowns at the stand level (Scott & Reinhardt, 2001).

Canopy fuels are defined as all burnable materials, which include live and dead foliage, lichen, and redundant stem and branchwood located in the upper forest canopy (Chuvieco & Congalton, 1989). Canopy fuels are important inputs for fire behavior models that predict crown fire behavior and spread (Scott & Reinhardt, 2001). Therefore, fire managers need more precise spatially explicit information about the fuels they manage. Canopy bulk density (CBD) and canopy base height (CBH) are the two main canopy fuel parameters (illustrated in Fig. 3.1) needed to predict crown fire spread (Van Wagner, 1977; Finney, 1998; Van Wagner, 1993). CBD is defined as the density of available canopy fuels, i.e. a measure of the amount of fuel contained per unit of canopy volume (Scott & Reinhardt, 2001; Hall & Burke, 2006). The CBD is a bulk

density of the whole stand, not a bulk density of an individual tree. CBH is defined as the vertical distance between the surface and live canopy fuel layer (Cruz et al., 2003; Kilgore & Sando, 1975; McAlpine & Hobbs, 1994; Van Wagner, 1977).

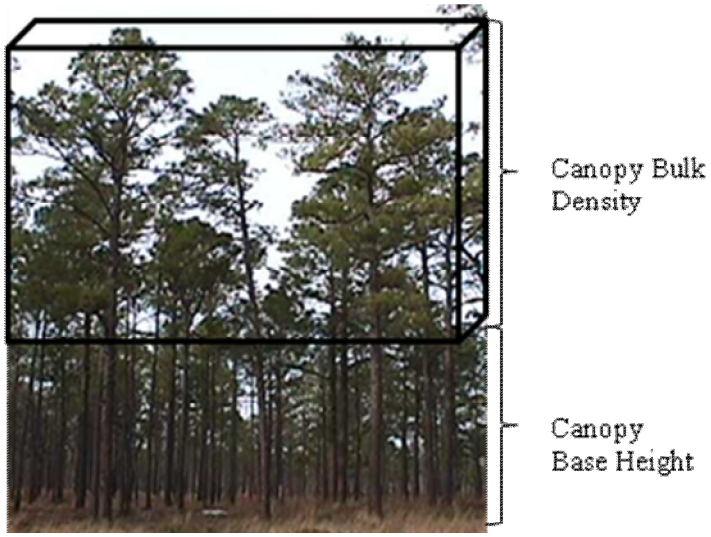

Fig. 3. 1. Two main canopy fuel parameters, CBD and CBH.

The CBD and CBH are important inputs for crown fire simulation models such as NEXUS and FARSITE (Finney, 1998). Assumptions are made when calculating CBD in regards to crown shape and the vertical distribution of foliage and/or branchwood within the tree crown. Of CBD and CBH, CBD is the most important canopy fuel parameter because active crown fires burn the entire surface-canopy fuel complex (Hall & Burke, 2006). However, CBH is also important since it may carry a surface fire to the crown.

In practice, CBD has never been directly measured in the field. One common way to estimate CBD is to divide an estimate of foliage biomass by an estimate of the canopy volume (Riano et al., 2003). This equation was used as a basis for creating a more specific and effective formula to estimate CBD canopy fuel for loblolly pines in this study. Some studies only estimated foliage biomass (i.e. Riano et al., 2003; Ranson et al., 1997) and ignored the branchwood component when estimating CBD. However, the branchwood component significantly contributes to crown fires to crown fire initiation and spread and therefore needs to be included in the estimation of available canopy foliage biomass (Jenkins et al., 2003). They collected all the available regression equations (over 2,500) in the literature and developed national scale total aboveground and component biomass regression equations for tree species in the USA. They developed estimators for five tree components: total aboveground, foliage, coarse roots, merchantable stem wood, and bark. In our study, the total aboveground and foliage biomass equations for loblolly pine trees were used. The foliage biomass equation includes both foliage and branchwood tree components. The ratio of foliage biomass to crown volume has been widely used by many researchers; however, the type of species has been ignored.

The CBD and CBH have been modeled for various species using allometric equations to predict crown fire behavior and spread for different regions of the U.S. However, none of those studies used species-specific equations for calculating crown volume and foliage biomass when calculating CBD at stand level. Species type plays an important role in calculating the CBD canopy fuel parameter (Baldwin & Peterson,

1997; Brown, 1978). Crown shape is an important determinant of crown volume (Baldwin & Peterson, 1997). Crown shape varies by species, if follows that species-specific CBD models should improve the prediction of CBD. There is a need to accurately predict the crown shape for specific species. Many studies use an assumption for crown shape and crown volume equations accordingly (i.e., Hall and Burke, 2006; Riano et al., 2003; Monserud & Marshal, 1999; Andersen et al., 2005). These assumptions tend to result in the over estimation of crown volume, because they include the space occupied by the canopy fuels (foliated) and the space not occupied by the canopy fuels (non-foliated) in the tree crown (Fig. 3.2a). In this study, using the equations from Baldwin and Peterson (1997), crown volume for loblolly pines was estimated by considering only the space occupied by the canopy fuels (Fig. 3.2b).

(a) (b)

Fig. 3.2. (a) Crown volume considering both non-foliated and foliated area, (b) crown volume considering only foliated area.

Unlike tree crown base height (CrBH), CBH is a complex stand-level variable that is not easily measured in the field (Van Wagner, 1993). One of the assumptions made when estimating CBH is that the canopy biomass is distributed uniformly within the canopy stand, which is unlikely even in stands with simple structures (Scott & Reinhardt, 2001). These assumptions can lead poorly defined CBH and CBD (Sando & Wick, 1972; Hall & Burke, 2006). Neither the lowest crown base height in a stand nor the arithmetic average of crown base height is likely to be representative of the stand as a whole. Therefore, Lorey's mean height was used in this study to calculate CBH. This method weights the contribution of trees to the stand height by their basal area by allowing the bigger trees to contribute more to the mean (Philip, 2002). The key in defining CBH for the purpose of modeling fire behavior is, for a given stand, to choose that height at which a fire is likely to move from the surface to the canopy and then to be carried by the canopy. These depend on many factors including fire intensity and wind speed. Fire has a spatial component so it is unlikely that the best choice is the lowest CBH as the occurrence of fire under that particular tree is less likely than it is under other trees in the stand. It is also unlikely to be the arithmetic average of the CBH.

The overall objective of this chapter was to estimate CBD and CBH for loblolly pines, at the plot level using both allometric equations and CrownMass/FMAPlus software. The CrownMass/FMAPlus software is most commonly prograsm used by fire managers to estimate CBD and CBH.

The allometric equation results were compared with those of CrownMass outputs for validation. An additional objective was to produce a canopy fuels map for the Huntsville, Texas region since no such map was available for use by fire managers.

Materials and Methods

Study Area

The study area is located in eastern Texas near Huntsville, covering about 47.15 km² (approximately 4800-ha) and contains part of the Sam Houston National Forest. Vegetation in the study area comprises upland, bottomland hardwoods, coniferous, old growth pine stands, mixed stands, brushes, upland and bottomland hardwoods, and open ground with fuels consisting of grasses. The study area is flat with average elevation is about 90 m. Fig. 3.3 represents the high-resolution (2.5 m x 2.5 m) multispectral QuickBird image of the study area. Yellow marks on the image illustrate the locations of field plots within the study area.

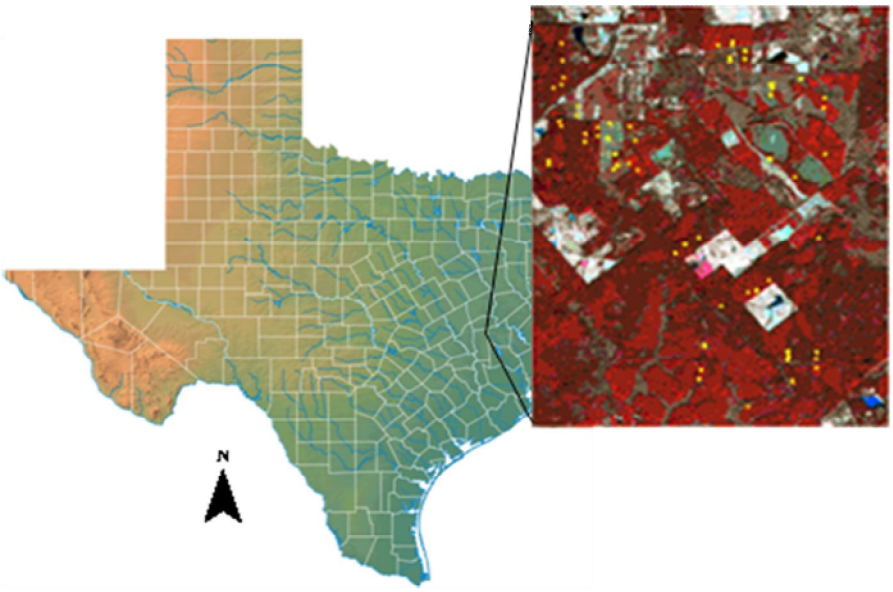

Fig. 3. 3. Map of Texas and a QuickBird image indicating the location of the study area, with field plot locations.

Processing Approach

The overall steps of this study are illustrated in Fig.3.4.

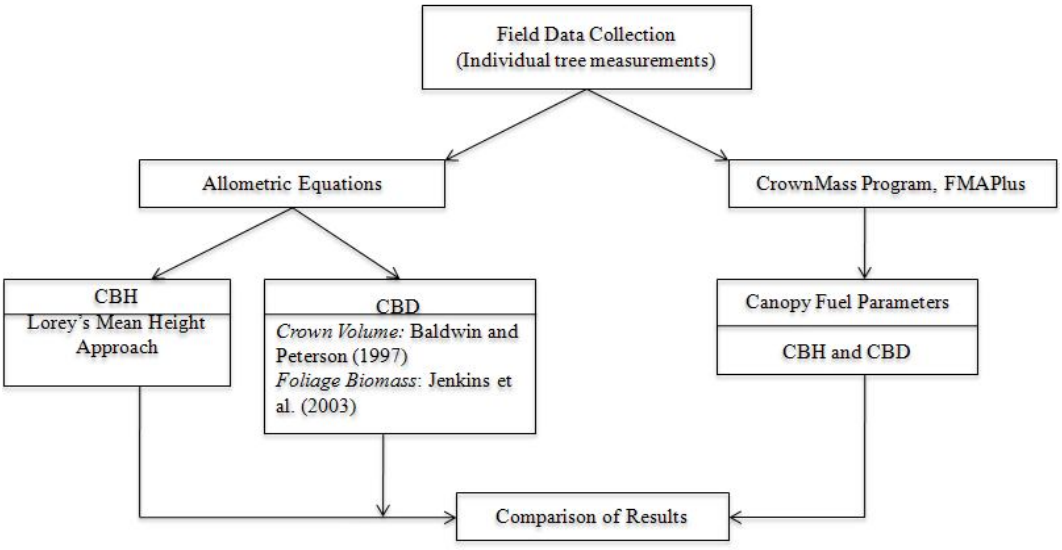

Fig. 3.4. The flowchart for steps used in this study.

Field Data Collection

Field data were collected from 50 plots between May 2004 and July 2004. Ground reconnaissance was used to identify the potential plot locations in Huntsville, Texas. Plot locations were determined by specialists from the Texas Forest Service taking into account: (1) ease of access to each plot; (2) land ownership (private or federal); and (3) covering a variety of vegetation cover types. Circular plots of two different sizes, a radius of 11.35 m (37.24 ft) covering a 404.7 m^2 (1/10th acre) and a smaller plot size of 40.468 m^2 (1/100-acre) with a radius of 3.59 m (11.78ft), were used in this study. The smaller plot size was used in the young unthinned loblolly pine plantations. The plot center coordinates were recorded with a GeoExplorerXT and were differentially corrected with Trimble's Pathfinder software. Inside of each plot boundary, the following parameters were measured for each tree: diameter at breast height (dbh), total tree height, crown base height, and crown class. In order to map each tree's location, distance (m) and azimuth from center of the plot were measured, starting from north and progressing clockwise. A Haglöf Vertex III hypsometer was used to measure total tree height and crown base height. Crown base height was measured as the distance from ground to the first live branch or whorl. A diameter tape was used to determine each tree's dbh. The Kraft system was used to classify each tree's crown: dominant, co-dominant, intermediate, and suppressed (Mutlu et al., 2008a). Using a hemispherical (fisheye) lens, canopy cover was recorded with upward- looking photographs taken from the center point. Table 3.1 provides general descriptions of the 50 plots.

Table 3.1
Descriptions of 50 plots in our study area.

			DBH (cm)			CBH (m)			TH (m)			% basal area	
Plot#	Size	#Trees	Ave	Min	Max	Ave	Min	Max	Ave	Min	Max	Pine	HW
H_1	1\10	24	16.2	2.3	25.9	8.4	0.9	11.9	12.2	1.5	17.9	0.99	0.01
H_2	1\10	25	15.8	3.0	29.2	7.7	1.4	12.0	11.7	1.8	19.4	0.96	0.04
H_3	1\10	35	13.1	2.8	23.9	7.2	0.3	13.1	10.8	0.9	18.4	0.97	0.03
H_4	1\10	29	14.2	3.3	28.4	5.5	0.4	11.4	11.2	1.4	17.4	0.97	0.03
H_5	1\10	27	13.7	4.3	41.1	5.7	0.9	10.9	11.1	5.0	19.3	0.79	0.21
H_6	1\10	38	15.7	3.6	47.8	6.4	2.0	12.2	10.7	3.9	20.8	0.95	0.05
H_7	1\100	11	11.8	3.0	18.8	4.7	1.6	5.8	9.8	3.6	14.1	0.97	0.03
H_8	1\100	4	3.4	2.5	4.3	0.2	0.2	0.5	2.2	2.1	2.4	0.75	0.25
H_9	1\100	4	2.6	1.8	3.0	0.2	0.2	0.2	2.1	2.0	2.2	100.00	0.00
H_13	1\100	8	13.7	4.3	24.9	6.8	3.5	11.6	10.8	5.4	15.8	0.93	0.07
H_14	1\10	9	13.7	6.6	19.1	7.3	5.7	9.3	10.8	8.8	13.1	0.94	0.06
H_15	1\10	32	17.6	4.8	38.9	9.1	4.0	16.0	14.6	5.1	27.3	0.86	0.14
H_16	1\10	22	17.0	6.1	32.3	8.1	2.3	17.2	13.5	2.9	27.1	0.49	0.51
H_17	1\10	35	17.9	4.3	66.0	7.1	1.4	21.1	12.7	2.7	37.1	0.85	0.15
H_18	1\100	9	13.9	6.4	16.3	6.0	4.2	7.1	10.7	7.7	12.0	0.55	0.45
H_19	1\10	25	19.8	7.1	48.3	8.5	3.2	17.8	14.0	6.0	26.6	0.33	0.67
H_21	1\10	13	31.3	11.4	39.9	16.5	3.1	21.5	25.2	11.5	29.5	0.94	0.06
H_22	1\10	8	34.1	12.7	78.5	13.3	8.8	19.3	23.5	16.8	32.5	100.00	0.00
H_23	1\10	8	29.5	9.4	64.3	11.9	4.5	21.5	20.6	8.2	31.1	100.00	0.00
H_24	1\10	25	27.9	5.8	65.8	9.3	3.1	25.9	16.8	7.3	37.5	0.73	0.27
H_25	1\10	11	13.2	3.8	29.7	7.6	2.5	11.2	12.2	4.6	17.8	0.73	0.27
H_26	1\10	43	15.0	4.3	33.5	9.3	3.5	14.2	13.5	4.6	22.2	0.94	0.06
H_29	1\10	7	36.3	13.7	58.2	9.5	2.9	13.3	19.6	6.7	27.5	100.00	0.00
H_30	1\10	5	51.6	29.2	72.9	11.5	2.7	17.5	24.9	15.0	28.6	0.89	0.11
H_31	1\10	13	50.1	36.8	72.6	16.4	5.5	23.4	32.8	24.9	37.2	0.75	0.25
L_1	1\100	10	8.5	3.3	17.5	4.3	2.4	7.6	6.4	4.6	10.7	0.97	0.03
L_2	1\100	5	11.9	4.1	17.8	6.6	2.7	10.7	10.0	3.4	15.5	0.85	0.15
L_3	1\100	11	14.8	6.9	38.1	7.8	2.2	10.9	12.4	6.6	19.8	100.00	0.00
L_4	1\100	10	13.7	7.6	21.1	9.5	2.3	12.2	13.8	10.7	16.5	0.95	0.05
L_5	1\10	41	14.9	5.1	51.6	7.0	1.5	16.8	10.6	1.5	22.9	0.66	0.34
L_6	1\10	33	16.9	5.8	72.4	6.0	1.8	18.3	12.2	6.1	33.5	0.45	0.55
L_7	1\100	7	5.1	4.1	6.4	0.3	0.3	0.3	2.6	2.6	2.6	100.00	0.00
L_8	1\100	3	3.6	2.8	4.6	0.3	0.3	0.3	2.6	2.4	2.7	100.00	0.00
L_9	1\100	4	4.1	2.8	5.1	0.3	0.3	0.3	2.3	2.1	2.6	100.00	0.00
L_12	1\10	39	19.8	10.9	31.8	9.8	2.1	12.2	13.6	9.1	16.8	0.91	0.09
L_13	1\10	6	41.8	36.1	49.3	14.9	11.3	17.0	22.5	22.1	23.1	100.00	0.00
L_14	1\10	23	22.3	15.5	27.2	11.5	9.6	14.8	18.5	15.1	20.4	100.00	0.00
L_15	1\10	16	21.5	5.6	37.8	9.2	2.7	11.0	16.2	7.1	18.6	0.99	0.01
L_16	1\100	6	12.7	5.8	16.0	3.0	1.9	5.1	8.0	5.7	9.3	100.00	0.00
L_17	1\100	11	10.9	5.1	16.0	2.9	1.1	4.7	8.2	4.8	9.3	0.95	0.05
L_21	1\10	57	19.5	6.9	28.7	11.3	4.3	13.9	16.2	5.3	19.0	100.00	0.00
L_22	1\100	5	20.3	14.0	27.9	12.0	10.3	13.1	18.1	14.9	19.7	100.00	0.00
L_23	1\100	6	16.9	9.7	20.8	10.7	6.9	12.3	14.9	7.6	17.2	100.00	0.00
L_25	1\100	5	15.6	6.4	24.4	8.1	6.4	9.2	14.1	9.8	17.4	0.90	0.10
L_26	1\100	3	18.7	16.0	20.8	7.8	6.8	8.3	15.6	15.4	15.7	100.00	0.00
L_27	1\10	13	27.3	7.6	61.0	10.0	2.1	19.8	19.7	7.2	32.7	0.84	0.16
L_28	1\10	11	27.3	4.6	44.7	6.7	1.5	13.7	14.3	3.7	22.3	100.00	0.00
L_29	1\10	12	24.8	10.4	43.2	9.5	3.0	15.1	17.0	9.1	22.3	100.00	0.00
L_30	1\10	8	27.8	11.7	45.7	9.1	3.7	20.0	17.9	6.9	30.1	0.81	0.19
L_31	1\10	38	19.4	6.4	45.7	8.4	2.3	20.2	15.3	4.6	30.1	0.86	0.14

Estimation of CBD and CBH Fuel Parameters

The CBD and CBH on all 50 plots located in the study area were estimated from a set of allometric equations and the CrownMass program in the FMAPlus software (FMAPlus3, 2003).

Estimating Canopy Fuels Using Allometric Equations

Crown bulk density (CrBD) is defined as the available biomass of the crown per unit volume of crown space (Reinhart et al., 2006; Cruz et al., 2003). CrBD was calculated by dividing predicted forest foliage biomass by predicted crown volume for loblolly pines (Riano et al., 2003) as follows:

$$CrBD = \frac{FB}{CV}\left(\frac{kg}{m^3}\right) \tag{1}$$

where FB and CV are the tree's foliage biomass and crown volume, respectively.

Jenkins et al. (2003) developed equations for predicting total aboveground biomass (equation 2) and foliage biomass (equation 3) for loblolly pine trees. The dbh was used in all the equations to estimate aboveground and tree component biomass. Their foliage biomass equation includes both foliage and branchwood components.

$$Bm = exp(\beta_0 + \beta_1 \ln(dbh)) \tag{2}$$

where Bm is total aboveground biomass (kg) for trees 2.5 dbh and larger, dbh is diameter at breast height (cm), Exp is exponential function, β_0 is set to -2.5356, and β_1 is set to 2.4349.

$$FBratio = Exp(\beta_0 + \frac{\beta_1}{dbh}) \tag{3}$$

where FBratio is foliage biomass ratio to total aboveground biomass for trees 2.5 cm dbh and larger, β_0 is equal to -2.9584, and β_1 is equal to 4.4766.

As mentioned before, crown shape is the key to calculating crown volume. Baldwin and Peterson (1997) developed a crown model that considers both inner and outer shapes to predict the crown shape of loblolly pine forests, shown in Fig. 3.2. This is noteworthy because the inner shape was not accounted in previous studies. In their study, they assumed that the profile is a simple balanced vertical cross sectional that involves outer and inner profile functions. A second degree polynomial was used to model outer profile and the crown tip was set to zero. A straight line model was used for inner defoliated cone-shaped area of the tree. Using their models and equations, maximum crown radius and its height, crown volume, and crown surface area can be determined. Their model can approximate a cone-shape crown. The crown volume equation they developed specifically for loblolly pine trees is given by:

$$CRVOL = \pi FL[3b_1^2 - 5b_1b_2 + \frac{b_2^2}{3} - 4\ln(2)\times(b_1^2 - 2b_1b_2) + \frac{b_3^3}{3b_4}] \tag{4}$$

The quantities b_1 through b_4 are defined by sub-models.

b1 = -4.5121 + 0.5176DBH + 4.3529R,
b2 = 4.4749 – 0.0175A – 0.4985DBH – 6.0414R,
b3 = 0.0168DBH + 0.0155FL, and
b4 = -0.0233dbh,

where A, R, and FL are the tree's are, crown ratio, and foliated crown length, respectively.

In equation 4, foliated crown length (FL) was calculated as total tree height minus crown base height obtained from the field data. Crown ratio was calculated as the ratio of crown length to total tree length. Site index and height information are needed to determine the age of a tree (A), necessary for equation 4. Stukey (2009) developed equation (5) to determine the age for the loblolly pine trees in our study area at base age 25.

$$A = \mathrm{e}^{\left(\frac{(TH + 0.453 \times SI)}{0.441 \times SI}\right)} \tag{5}$$

where TH is tree height and SI is site index.

Site index is described as the average height of the dominant and co-dominant trees on the site at a given base age (Avery and Burkhart, 1987). Site index for our study area was obtained from Soil Survey Geographic (SSURGO) data. The study area has site

indices of 15.2 m (50 ft), 21.3 m (70 ft), 24.4 m (80 ft), 25.6 m (84 ft), and 27.4 m (90 ft) at 25 years.

By applying the equation (1), we obtained only CrBD at tree level not the CBD at stand level. From now on, CBD estimated from allometric equations is named as $CBD_{AL.}$ The CBD_{AL} was calculated as:

$$CBD_{AL} = \frac{\sum FB}{\sum CV} \tag{6}$$

Lorey's mean height, also called weighted mean height approach, was used to calculate CBH in this study. This is a commonly used method in the US. In our study, tree's CrBH value was multiplied by tree basal area for all trees within the plot boundaries, and then divided by the basal area of stand (equation 7). This method weights the contribution of trees to the stand height by their basal area by allowing the bigger trees to contribute more to the mean (Philip, 2002). Because of the silvicultural treatments, e.g. thinning from below, harvesting smaller trees, and mortality of trees, Lorey's mean approach is more stable than unweighted (arithmetic) mean approach (Brack, 1999). From now on, CBH estimated from Lorey's mean height equation is named as $CBH_{LH.}$

$$CBH_{LH} = \frac{\sum (BA \times CrBH)}{\sum BA} \tag{7}$$

where CBH_{LH} is canopy base height estimated using Lorey's mean height eqaution at plot level, CrBH is crown base height at individual tree level, and BA stands for basal area.

Estimating CBD and CBH Using CrownMass Program

For comparative purposes CBD and CBH were also calculated using the CrownMass program within FMAPlus software (FMAPlus3, 2003). CrownMass is based on the work of Beukema et al. (1999), Rothermel (1972), Andrews (1986), and Finney (1998). The program accepts and processes overstory data and estimates the fire behavior and fire effects. Required inputs are tree diameter at breast height, tree height, tree crown ratio and tree structural stage. Based on the tree list data, the software determines the canopy fuel loading for the needle and the 1-hour timelag live/dead fuel categories. The program assumes that the distribution of crown loading is vertically uniform within the canopy. Each tree is divided into one-foot (0.3048 m) vertical segments from the tree's crown base height to the tree's total height by the program (FMAPlus, 2003). The loading for each foot segment is calculated by summing the loading contributions to that segment from all trees within the stand. A running mean of these values is calculated and the maximum running mean value is used by this software as CBD (FMAPlus, 2003). The CBH is determined by CrownMass as the lowest segment where the running mean segment bulk density is greater than the minimum crown bulk density, 0.0111 kg/m³ (33 lbs/acre/foot). We will refer to the CrownMass estimators of CBD and CBH as CBD_{CM} and CBH_{CM}, respectively.

Results and Discussion

The allometric equations always produced higher values for average CBD (Fig. 3.5) and CBH (Fig. 3.6). The comparison of calculated general statistics for canopy fuel parameters is presented in Table 3.2.

Table 3.2
General statistics for computed CBD and CBH (Min, minimum value; Max, maximum value; Ave, average; St. Dev., standard deviation).

	CBD (kg/m3)		CBH (m)	
	CBD_{AL}	CBD_{CM}	CBH_{LH}	CBH_{CM}
Min/Max	0.03/0.47	0.006/0.18	0.1/24.3	0.21/23.1
Ave/St.Dev.	0.18/0.10	0.07/0.05	10.6/5.1	9.1/4.9

The CBD values calculated using the allometric equations method varied between 0.03 kg/m³ (min) and 0.47 kg/m³ (max) with an average of 0.18 kg/m³. In comparison, CBD values obtained from the CrownMass program ranged between 0.006 kg/m³ (min) and 0.18 kg/m³ (max) with an average of 0.07 kg/m³. The average difference between the two methods is 0.11 kg/m³ and using allometric equations results in a value approximately 2.5 times greater than the value estimated by the CrownMass program. The CBD estimates from our method exceeded CrownMass program estimates by 157%. In our study, CV was calculated by considering only the space occupied by the canopy fuels and therefore generated results with higher CBD values over the entire study area. In previous studies, crown volume was over estimated by considering both space occupied and space not occupied by the canopy fuels in the tree crown (Keane et

al., 2000; Cruz et al., 2003; Riano et al., 2003). However, in this study crown volume was calculated considering only the space occupied by the canopy fuels and the shape of the loblolly pine tree crowns. Therefore, comparatively low crown volume values were obtained. Further, dividing the foliage biomass by a smaller crown volume resulted in higher CBD values. Therefore, if space not occupied by the canopy fuels were included in our calculations, CBD values would be closer to the results of the CrownMass program.

The recent study by Roccaforte et al. (2008) compared three different methods of calculating the CBD canopy fuel parameter for three different years over the same study area: 1870, 1996-97, and 2003. The CBD parameter used in this study is described by Brown (1978), Fule et al. (2001), and Cruz et al. (2003). Roccaforte et al. (2008) concluded that for the same dataset and area, average CBD for given areas in 1870 was 0.01 kg/m³ from Fule et al. (2001), 0.02 kg/m³ from Brown (1978), 0.03 kg/m³ from Cruz et al. (2003). In addition to the results from 1870, the following CBD values were obtained in 1996-97: 0.05 kg/m³ from Fule et al. (2001), 0.12 kg/m³ from Brown (1978), and 0.23 kg/m³ from Cruz et al. (2003). Finally, in 2003, CBD was 0.05 kg/m³ from Fule et al. (2001), 0.13 kg/m³ from Brown (1978), and 0.22 kg/m³ from Cruz et al. (2003). As a result of Roccaforte et al. (2008) study, all the CBD results were not similar at all. Brown (1978)'s estimates exceeded Fule et al. (2001)'s estimates by 184–268% and Cruz et al. (2003)'s estimates exceeded Fule et al. (2001)'s estimates by 153–491%. For the same area and the same dataset, Scott (2008) ran two different canopy fuel calculation software, FuelCalc and FMAPlus, respectively. The differences between

these two softwares were larger than they expected. Based on their conclusion, FMAPlus is over-predicting the canopy fuels compared to FuelCalc software. As a result, there is apparently no substantial difference between the results from our method and the CrownMass program. Therefore, CBD values obtained from allometric equations do not seem unreasonably high. The distribution of average CBD values obtained from two different methods is presented in Fig. 3.5 in this study.

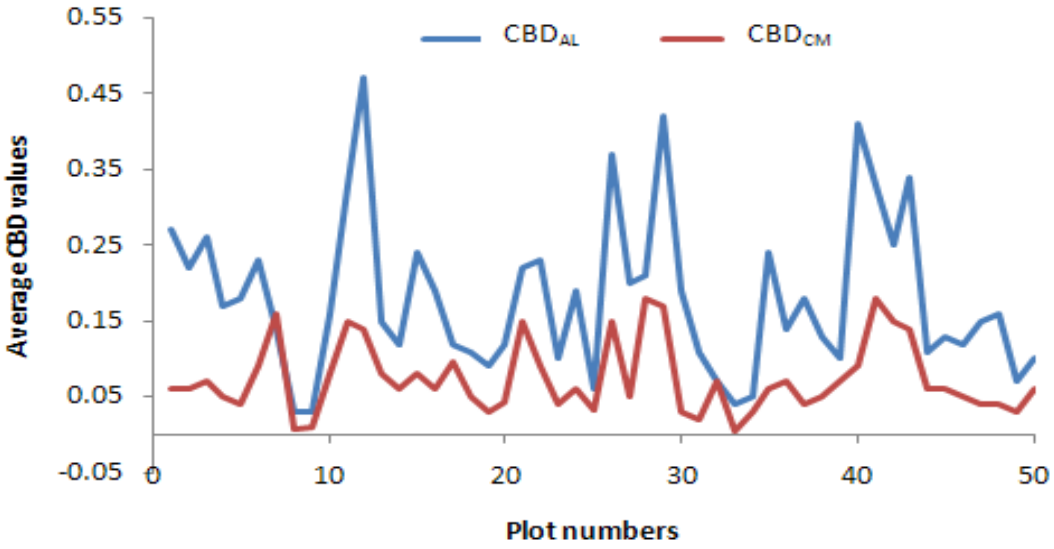

Fig. 3.5. Distribution of the average CBD values for loblolly pine forests.

The height values of CBH obtained from Lorey's weighted height varied between 0.1 m (min) and 24.3 m (max) with an average height of 10.6 m. The height values of CBH obtained from the CrownMass program varied between 0.21 m and 23.1 m with an average height of 9.1 m. For CBH, Lorey's weighted height estimates

exceeded CrownMass program estimates by 16%. Lorey's mean height approach is one of the most accurate ways of calculating CBH without using any program, because the average height and/or the lowest crown base height will not represent the stand as a whole. The average height results obtained from two different methods are quite close to each other and our estimation is 1.16 times more than that estimated by the CrownMass program. The distribution of average CBH values obtained from two different methods is presented in Fig.3.6 in this study.

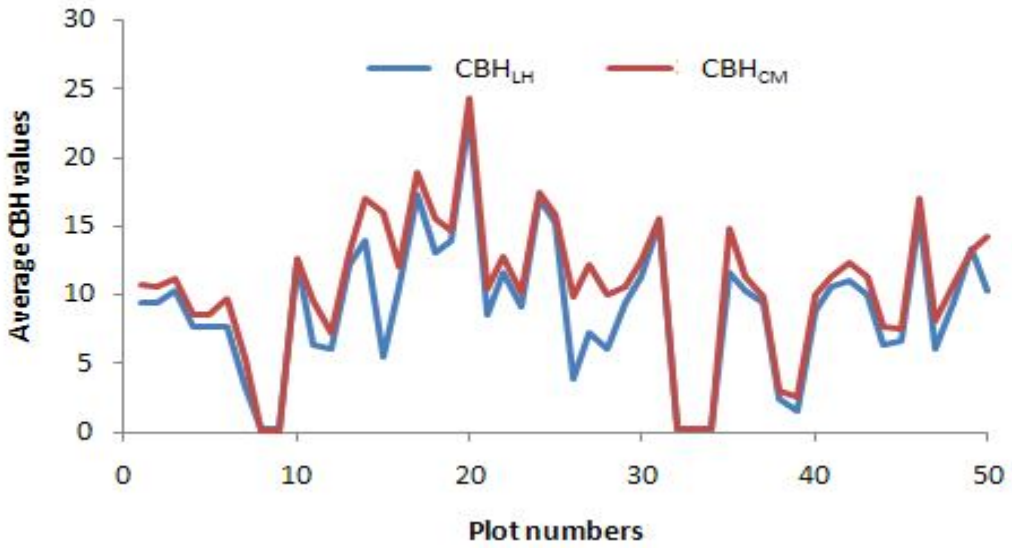

Fig. 3.6. Distribution of the average CBH values for loblolly pine forests.

Conclusions

When a wildfire burns out of control, the size of the losses can be almost inestimable. Improving the accuracy of mapping fuel loads is essential for fuel management decisions and for explicit fire behavior prediction for real-time support of suppression tactics and logistics decisions. Fire managers need more accurate fire behavior predictions, and benefits can be gained from improving key canopy fuel parameters such as canopy height, canopy bulk density, and canopy base height (Pyne et al., 1996).

The objective of this study was to improve and incorporate suitable allometric equations to estimate CBH and CBD canopy fuel parameters at stand level, specifically for loblolly pine plantations. The CrownMass program was also used to estimate the same parameters as those produced from our calculations. In this way, we were able to assess our results. The results of this study show that our approach has great potential for becoming a standard method for estimating CBD and CBH canopy fuel parameters for loblolly pine trees in eastern Texas. Our values compared reasonably well with the CrownMass program estimates and yet highlight the differences due to adopted definitions of biomass and crown volume. The CBD results showed the effect of including the branchwood tree component in defining foliage biomass because foliage and branchwood account for the majority of CBD estimates. Furthermore, these components are considered the primary fuels for crown fires (Keane et. al., 2005). Our results also highlights that consideration of crown shape is an important aspect when defining crown volume and CBD, a key canopy fuel parameter.

A digital elevation model, slope, aspect, surface fuel map, CBH, and CBD are required to run FARSITE. Many fire managers do not have the surface fuel map, canopy bulk density, or canopy base height data layers. Instead, they are required to use very coarse estimates of these inputs. There has been no reliable, accurate, and simple method for estimating these parameters and thereby providing high quality input for FARSITE crown fire modeling. The same problem exists with regards to inputs for other fire simulation software packages such as BehavePlus and FlamMap. It is imperative that these datasets be delivered in formats suitable for input to fire simulation systems used by fire managers. In addition, satellite remote sensing technology has been proven to estimate forest inventory data over large areas (Riano et al., 2003; Ranson et al., 1997). Previously, the estimation of canopy fuel parameters and the generation of canopy fuel maps from remote sensing required ground inventory data. Estimators CBD_{AL} and CBH_{LM} can be used as ground inventory data to estimates these parameters from remote sensing technology and then spatial explicit maps can be easily generated.

This study also highlights that canopy fuel parameters, CBD and CBH, can be easily derived using allometric equations. There is no published study on calculating CBD for this area. Fire managers can use our approach for loblolly pine trees in eastern Texas and they do not need to purchase any software such as FuelCal and/or CrownMass to derive these parameters.

CHAPTER IV

ESTIMATING CANOPY BULK DENSITY AND CANOPY BASE HEIGHT FUEL PARAMETERS USING AIRBORNE LIDAR DATA

Introduction

Due to the increase of crown fires in the United States, crown fire behavior is an important consideration in fuel assessment for fire managers (Allen et al., 2002; Westerling et al., 2002). The accurate prediction of the potential risk of a crown fire is necessary for fire management activities and it may reduce the seriousness of crown fires (Pyne et al., 1996). All fire behavior properties are strongly related to fuel distribution (Mutlu et al., 2008b; Riano et al., 2003). Therefore, there is a need to characterize crown fuel parameters, such as canopy bulk density (CBD), canopy height, canopy volume, and canopy base height (CBH), for crown fire behavior. This chapter presents methods for deriving CBD, defined as the density of available canopy fuels (Cruz et al., 2003; Scott & Reinhardt, 2001; Hall & Burke, 2006), and CBH, defined as the vertical distance between the ground surface and live canopy fuel layer (Cruz et al., 2003; Kilgore & Sando, 1975; McAlpine & Hobbs, 1994; Van Wagner, 1977), using airborne lidar remote sensing technology.

Airborne lidar sensors are high resolution active remote sensing tools that use lasers to measure the distance between the sensor and an object (Wagner et al., 2004). These systems distribute thousands of laser pulses per second and measure the return time needed for each pulse sent from the sensor to reach the ground and reflect back to

the sensor (Naesset & Gobakken, 2005; Popescu, 2007). Lidar technology provides useful information on the three-dimensional structure of canopy surface and vegetation parameters, such as tree height, stem density, crown dimensions, volume, and biomass (Naesset & Okland, 2002; Nelson et al., 2003; Popescu et al., 2004). Aboveground biomass, foliage biomass, and crown volume are the main parameters required to derive CBD. Studies have shown that lidar can be used to derive these parameters for extended areas (Lefsky et al., 1999; Means et al., 1999; Popescu, 2007; Nelson et al., 2003). Applications of airborne lidar remote sensing for forest fire applications over large areas have been rapidly increasing in recent years, which have effectively improved estimates of canopy fuel metrics for wildfire behavior modeling (Popescu & Zhao, 2008). Therefore, lidar is a very valuable tool for the prevention, detection and mapping of wildland crown fires (Andersen et al., 2005; Means et al., 2000). This technology can be used for fire risk management to decrease crown fire risk and to reduce fire damage. In addition, airborne lidar datasets are becoming increasingly available and are less expensive than in the past. Thus, lidar is gaining popularity as a tool for natural resource management.

Previous studies have shown that airborne lidar remote sensing can be used to measure canopy structure to predict important aspects of stand structure which include aboveground biomass, mean diameter at breast height (dbh), stem density, stem volume, basal area, canopy cover, and CBH (Lefsky et al., 2002; Maclean & Krabill, 1986; Means et al., 1999; Nelson et al., 1984; Popescu & Zhao, 2008). These techniques also have been used for mapping the spatial distribution of forest surface fuels and canopy

fuel parameters (Mutlu et al., 2008a; Popescu & Zhao, 2008). Some studies also have shown the ability to transform lidar measurements to approximate common field measured parameters, including canopy cover, stand height, and vertical distributions of foliage density (Carreiras et al., 2006; Means et al., 1999). Airborne lidar is particularly valuable for measuring CBD because it can provide information about biomass, crown length, tree crown, tree height, and volume (Hyyppa et al., 2000; Lefsky et al., 2001; Popescu & Zhao, 2008). The CBD is an important canopy fuel parameter because programs such as FARSITE (Fire Area Simulator) use a threshold value of CBD for achieving and sustaining an active crown fire. The CBH layer is also important for determining the probability of fire transition from ground surface to tree crown.

FARSITE is the most commonly used decision-support system tool for wildfire modeling by fire managers all over the world. FARSITE requires a variety of inputs that can be derived from lidar data including elevation, slope and aspect, fuel model, canopy cover, tree height, CBH, and CBD, in addition to other inputs, such as temperature, wind direction, and wind speed (Finney, 1998).

Field measurement techniques are not standardized and consistently applied to assess the forest fuels, complicating the efforts to model fire behavior at the landscape scale. There is a need for a standardized and efficient approach for measuring crown fuels in forest stands that exhibit a wide variety of structural characteristics. Several key spatial data layers are required by FARSITE and they are often difficult to derive. These layers include: surface fuel model, canopy cover, CBD, and CBH. Crown fire data inputs are difficult to create; therefore, they are presented as “optional” in the FARSITE

software. Many fire managers do not have these important data layers and they are required to use very coarse estimates of these inputs or generalized assumptions. We employ a unique approach to derive these spatial data layers from airborne lidar data. There has been no reliable, accurate, and simple method for estimating these parameters and providing high quality inputs for FARSITE crown fire modeling. Some studies derived only CBD and CBH canopy fuel parameters (i.e., Cruz et al., 2003; Riano et al., 2003; Fule et al., 2004), but could not generate the maps needed for fire simulation software. Even though they derived these parameters, they did not have the other two key inputs required for FARSITE, which are canopy cover and surface fuel model maps. We derived these two inputs in our previous study, Mutlu et al. (2008a). None of the studies have developed all these important data layers for the same study area and run FARSITE to simulate the fire behavior. In contrast with other studies, our study group has developed all these spatial inputs with high accuracy maps for forested areas in Texas, and simulated fire growth and behavior. It is necessary to deliver these datasets to fire managers in formats suitable for use with fire simulation systems.

The overall aim of this chapter is to estimate the two critical forest canopy fuel parameters including CBH and CBD using airborne lidar data for loblolly pine trees in east Texas. More specific objectives were: (1) to develop a methodology for assessing CBD and CBH with lidar derived metrics by investigating several processing approaches including lidar point cloud metrics, height bins, and lidar-multispectral data fusion; and (2) to map CBD and CBH from airborne lidar for the entire study area.

Materials and Methods

Data

Three types of data were used in this chapter: field data, a multispectral Quickbird image, and airborne lidar data.

Field Data

Field data, also called ground inventory data, is required to derive CBD and CBH from the airborne lidar data. Field data collection and derivation of CBD and CBH were discussed in detail in Chapter III. The validation of airborne lidar data to retrieve forest parameters has been widely tested using field data (Riano et al., 2003; Hyyppa et al., 2001; Means et al., 2000; Naesset, 1997). In this study, field data were used to validate CBD and CBH canopy fuel parameters derived from airborne lidar data.

Multispectral Image

The multispectral Quickbird image used in this study (Fig. 4.1a) is a high resolution (2.5 x 2.5 m) satellite image in 2004. The major physical parameters of the Quickbird satellite are that the spatial resolution of the panchromatic band is only 0.61 m, and the spatial resolution of multispectral bands (blue, red, green, and Near infrared (NIR)) is only 2.44 m (DigitalGlobe, 2010). The Charge-Coupled-Device (CCD) sensor of QuickBird has 5 channels: the black and white (panchromatic) channel gets the spectrum at 445-900 nm; the other four multispectral channels cover the blue spectrum at 450-520 nm, the green spectrum at 520-600 nm, the red spectrum at 630-690 nm

wavelength, and the near-infrared spectrum at 760-900 nm wavelength (http://www.digitalglobe.com/index.php/85/QuickBird).

Lidar Data

Airborne lidar scanning data over an area of 6,474.9 hectare (25 square miles) was obtained in leaf-off condition during March 2004. The lidar system (Leica-Geosystems ALS40) recorded two returns per laser pulse, first and last. The horizontal accuracy is 20-30 cm and vertical accuracy for the mission is 15 cm. To allow a good penetration of laser shots to the ground and to decrease effects of row direction on loblolly pine plantations, two different flight line directions were designed. A total of 19 flight lines were obtained from East to West and a total of 28 flight lines were obtained from North to South in LAS file format over the study area. The average point density is 2.58 laser points/m² and the maximum point density is 39.84 laser points/m². The average distance between laser points is 0.62 m for the entire point cloud. Fig. 4.1b represents all 47 flight lines over the study area.

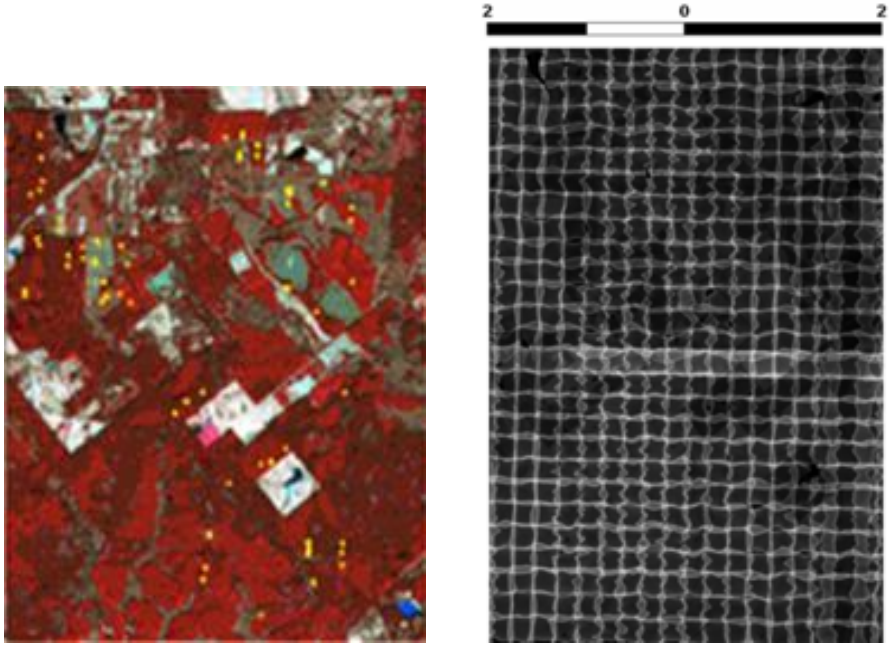

(a) (b)

Fig. 4.1. (a) Quickbird image and (b) airborne lidar flight lines over Huntsville, TX.

Processing Approach

The overall steps of this study are illustrated in Fig.4.2.

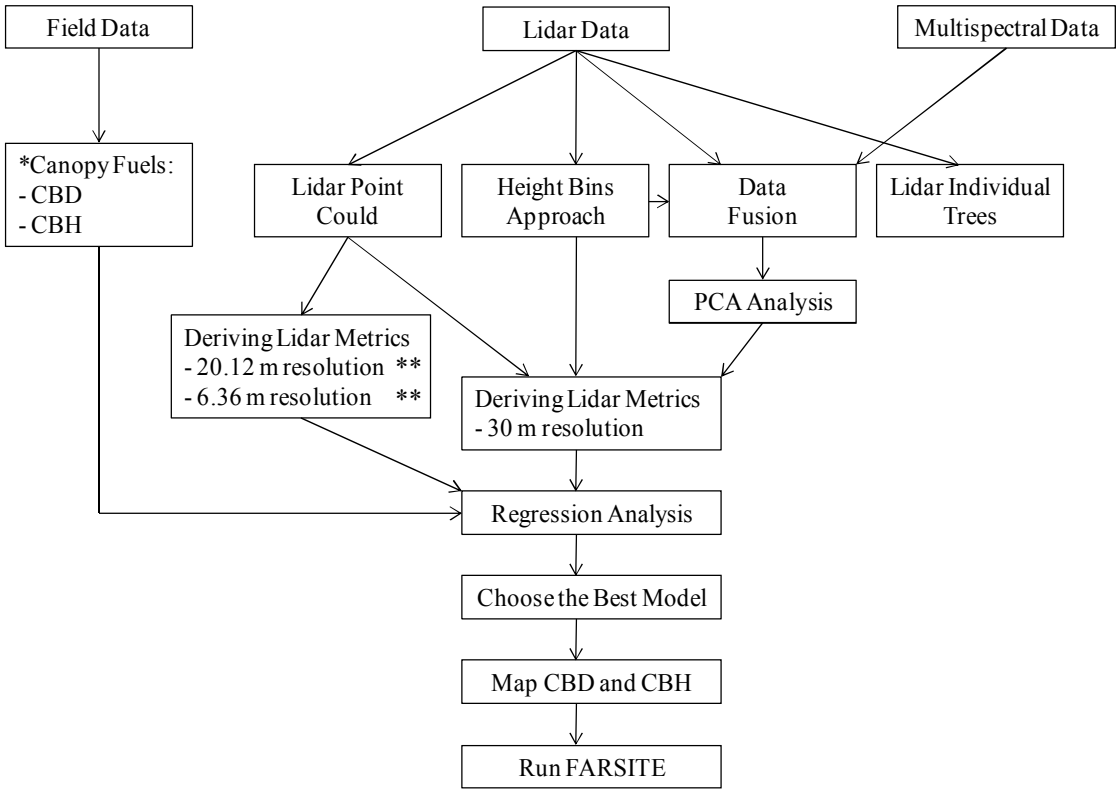

*Chapter III canopy fuel parameters (CBH and CBD) results were used as reference data
** 20.12 m and 6.36 m are the grid sizes equivalent to a 404.7 m² and 40.47 m² plot sizes, respectively.

Fig.4.2. A flowchart of the processing approach.

Height Bins Approach

The height bins approach was used to generate lidar multiband data from airborne scanning lidar data (Popescu and Zhao, 2008). The height bins approach makes use of the entire lidar point cloud. Lidar bins were created by counting the occurrence of the number of lidar points within each volume unit and normalizing by the total number of points. The percentage of lidar hits can be obtained for any height interval.

A total of eleven lidar height bins were obtained and illustrated in Fig. 4.3. The first four height bins are generated for 0.5 m height intervals to afford a better characterization of vegetation that defines surface fuels. The other bins are spaced at: Bin 5: 2.0-5.0 m, Bin 6: 5.0-10.0 m, Bin 7: 10.0-15.0 m, Bin 8: 15.0-20.0 m, Bin 9: 20.0-25.0 m, Bin 10: 25.0-30.0 m and the last bin is generated from laser hit above 30 m (Bin 11: >30.0 m). All the height bins were used in this study to derive CBH and CBD canopy fuel parameters.

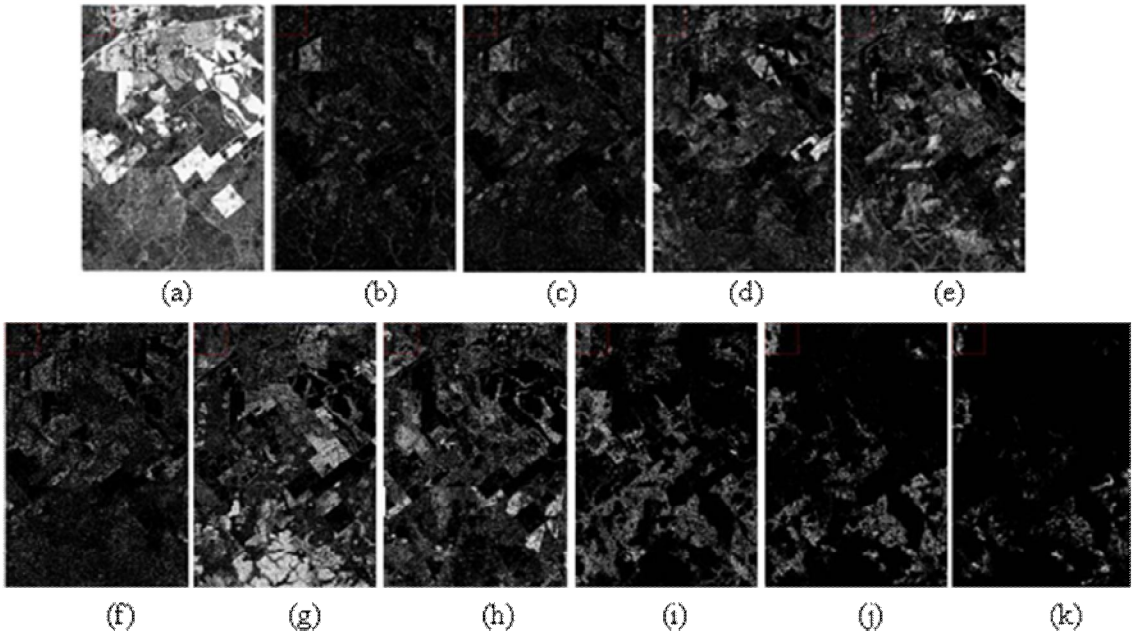

Fig. 4.3. Height bin images: (a) 0-0.5 m, (b) 0.5-1.0 m, (c) 1.0-1.5 m, (d) 1.5-2.0 m, (e) 2.0-5.0 m, (f) 5.0-10.0 m, (g) 10.0-15.0 m, (h) 15.0-20.0 m, (i) 20.0-25.0 m, (j) 25.0-30.0 m, and (k) >30.0 m.

Data Fusion and PCA Analysis

In this study, we created a new image by stacking the four bands of the QuickBird image with all the lidar height bins (bin 1 through bin 11). Data fusion deals with association, correlation, and combination of information and data from one or many sources (Llinas, 2002). The range of values for the height bins bands and the Quickbird image are different. The QuickBird data obtained from DigitalGlobe have 2048 possible intensity values for each pixel. Lidar height bins are the density of points at each height interval and ranged from zero to one. Therefore, data spanning 2048 values are normalized and rescaled to 0 to 1 value to avoid any bias because of the scale differences.

Principal Component Analysis (PCA) was applied to our stack image, which has fifteen bands. ENVI 4.5 (ITT, Boulder, CO) was used for layer stacking and PCA transformation. PCA is a statistical technique used to produce uncorrelated output bands, to segregate noise components, and to reduce the dimensionality of data sets by transforming a set of correlated variables into a new set of uncorrelated variables (Jensen, 2005). Basically, original data is transformed into a new set of data which may better capture the essential information. The PCA transformation is based on the variance and covariance of the data set (Jensen, 2005). The variance is a measure of the scatter or spread within one variable of the data set, and the covariance is a measure of the scatter between two variables of a data set (Smith, 2002). PCA reduces the dimensionality of the data and keeps the most significant part of the data.

Eigenvalues, variance, and eigenvector were extracted for each principal component (PC). Table 4.1 represents the percentage of total variance, eigenvalues, and cumulative variance explained by each PC. Each eigenvector represents a principle component. The first PC is defined as the eigenvector with the highest corresponding eigenvalue. The individual eigenvalues indicate the variance, the higher the value the more variance they have captured.

Table 4.1
Calculated percentage of total variance, eigenvalues, and cumulative variance explained by each principal component.

PCs	Eigenvalue	%of total variance	cumulative
PC1	0.124942	48.2299	0.482299
PC2	0.040637	15.6866	0.639165
PC3	0.032816	12.6676	0.765841
PC4	0.020207	7.8003	0.843844
PC5	0.01866	7.2031	0.915875

We used the first five components, which account for approximately 92 % of the total variance, to derive CBD and CBH canopy fuel parameters. Fig. 4.4 represents all the PCA components used in this study. It can be concluded that the first five principal components can replace the original fifteen bands of the stack image, while reducing the size of the data set, redundancy, and noise.

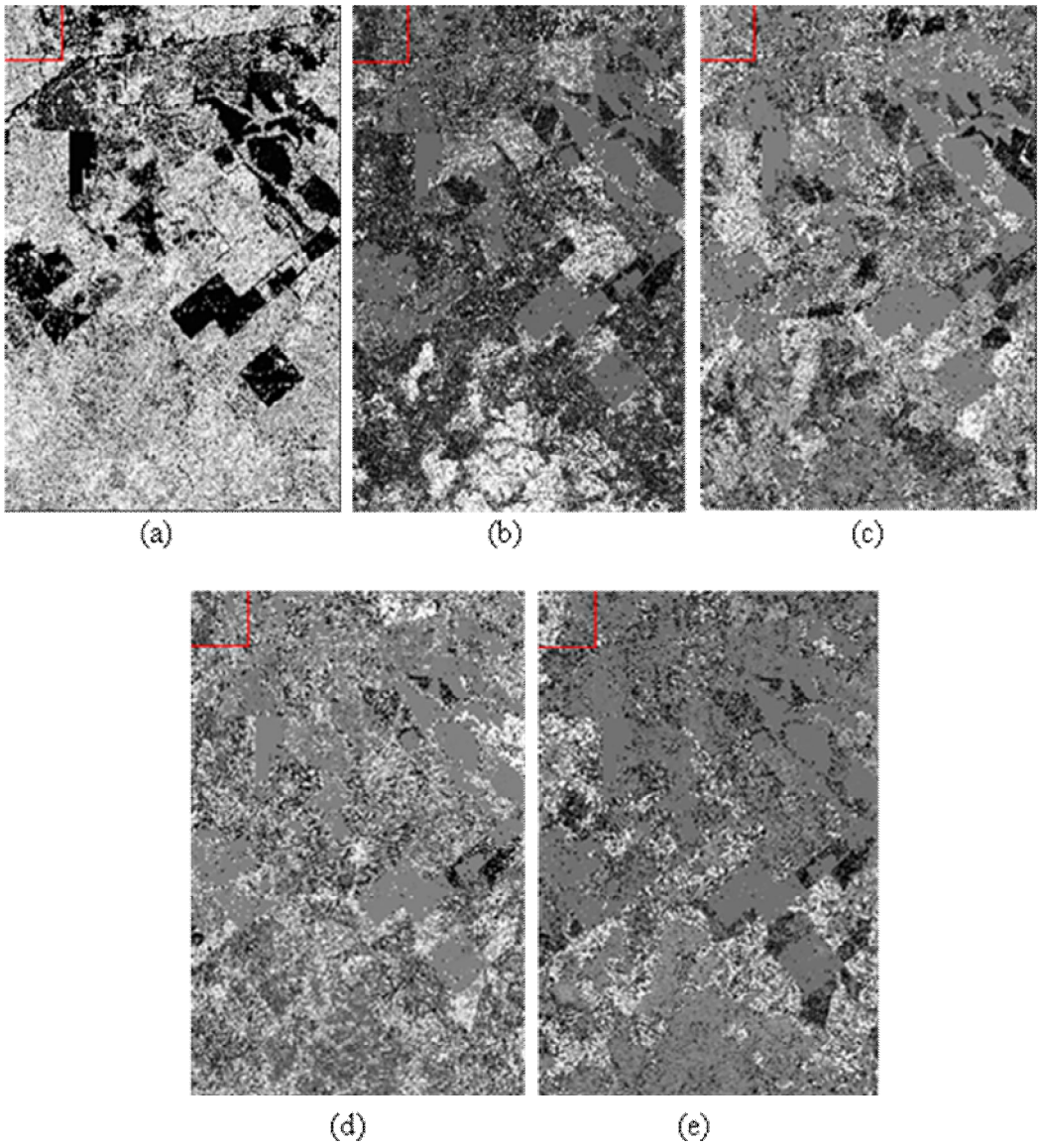

Fig. 4.4. The first five PCs: (a) PC 1, (b) PC 2, (c) PC 3, (d) PC 4, and (e) PC 5.

Estimating Canopy Fuel Parameters

We have a total of 50 plots with two different sizes: 33 of them are 404.7 m² ($1/10^{th}$ acre) and 17 of them are 40.47 m² ($1/100^{th}$ acre). The smaller plot size was selected because the loblolly pine trees in unthinned plantations are uniform and the

40.47 m² (1/100th acre) size was enough to represent the stand. Measuring the same type of stand using 404.7 m² (1/10th acre) plot size is economically expensive and time consuming. Four processing approaches were used to derive CBD and CBH canopy fuel parameters. First, two different datasets were used to derive these canopy fuel parameters from the entire airborne lidar point cloud at two different map spatial resolutions: (1) at 30 meter resolution, (2) at a grid cell size with an area equal to the actual plot size. Second, CBD and CBH were derived at plot level using an individual tree approach. Third, upper lidar height bins corresponding to the canopy were used to derive these canopy fuel metrics. Lastly, PCA components (data fusion) were used in this study.

Lidar Point Cloud Approach

Estimating Canopy Fuel Parameters at 30 Meter Resolution

First, pixel size was set to 30 m resolution, which is larger than the actual plot size, to derive all lidar metrics to compensate for any GPS errors when locating ground plots. Similar to studies of Naesset and Bjerknes (2001), Erdody and Moskal (2010), and Andersen et al. (2005), eight lidar metrics were derived from the lidar point cloud including: 25th, 50th (median), 75th, and 90th of height percentiles of laser pulses, maximum height, mean height, coefficient of variation (cv), and canopy density (D), calculated as the number of all returns above 2.5 m divided by the total number of all returns at 30 m. In addition, logarithmic transformation was applied to our metrics. The log transformation is used for normalizing the data, easier data visualization, and

correcting heteroscedasticity (Fox, 1997). This transformation also helps homogenize the variance over the sample data and equalizes the variance over the entire range of predicted *y* values (Sprugel, 1983). Including log-transformed metrics, we obtained a total of sixteen metrics at 30 m resolution.

Estimating Canopy Fuel Parameters at Actual Plot Size

In this step, canopy fuel parameters were derived at actual plot size. Same eight metrics derived at 30 m resolution were derived at 20.12 m ($1/10^{th}$ ac) and 6.36 m ($1/100^{th}$ ac) resolutions assuming plot center was accurately located at the center of the pixel. Centered shapefiles were created in ArcMap 9.1 for each individual plot location: 33 with 11.35 m radius for $1/10^{th}$ acre plots and 17 with 3.59 m radius for 1/100 acre plots. These plots were saved as ascii file format in order to open the point cloud of each plot in QTM (Quick Terrain Modeler) software. A digital elevation model (DEM) was created using QTM to interpolate the raw lidar data and used as true ground height above the sea level. Then, each plot point cloud was extracted from the total lidar point cloud using the "Clipping Panel" tool in QTM (Fig. 4.5) and saved as a text file for statistical analysis. The R (R Development Core Team, 2005) statistical software package was used to derive all the metrics, except the D metric. The QTM software was used to derive the D metric. After applying the log transformation to these metrics, we also obtained a total of sixteen lidar metrics in this section.

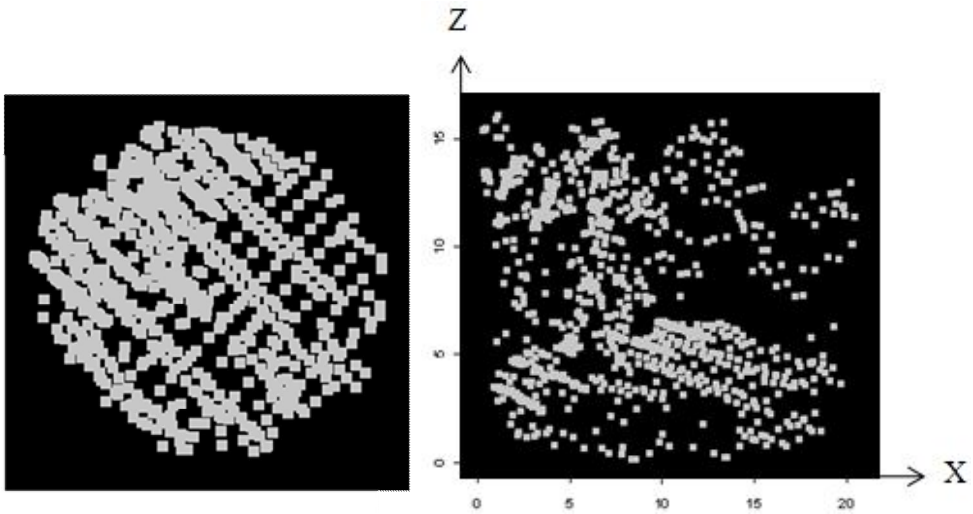

(a) (b)

Fig. 4.5. Two snapshots of the Plot# Hunt_6 (r =11.35 m) lidar point cloud from the QTM software from above (a) and a side (b), respectively.

Estimating Canopy Fuel Parameters at Plot Level Using Trees Captured by TreeVaw

In Chapter III, we used species-specific equations, adapted from Baldwin and Peterson (1997) and Jenkins et al. (2003), to derive CBD and Lorey's mean height approach to derive CBH at plot level. Field measurement inputs were used into these allometrics equations in Chapter III. Total tree height, crown ratio, foliage biomass, age, and crown length are necessary variables for our allometric equations to estimate crown bulk density (CrBD) at tree level and CBD at plot level.

Airborne lidar can be used to estimate all these variables. Instead of using field measured variables in these equations, we used variables derived from airborne lidar data using the studies of Popescu and Zhao (2008) and Stukey (2009). Popescu and Zhao (2008) used TreeVaw (Tree Variable Window) developed by Popescu and Wynne (2004) to extract tree heights and crown diameters at individual tree level in our study

area. Stukey (2009) used the results of Popescu and Zhao (2008) and Popescu (2007) to estimate dbh, CBH, and age of each individual pine tree for the same study area. Thousands of trees for the whole study area were identified by the TreeVaw software. The locations of plots and all the trees captured by TreeVaw were displayed in ArcGIS 9.2. Then, trees fallen in each plot boundaries were selected and a text file was created for further analysis. Initially, we had 50 plots, but we only used 41 out of 50 plots. Nine of the 50 plots could not be used since there was no tree captured by TreeVaw software within the plot boundaries. In addition, foliage biomass and crown length of each tree were estimated using dbh and total tree height data obtained from Popescu and Zhao (2008) and Stukey (2009), to calculate CrBD at individual tree levels and CBD at plot levels.

Estimating Canopy Fuel Parameters from Lidar Height Bins and Data Fusion Approaches

Seven upper lidar height bins (bin 5 through bin 11, Fig. 4.3) were used to derive CBD and CBH canopy fuel parameters. The first four lidar height bins were not used since they represent the surface fuels (Mutlu et al., 2008a). On each individual plot location, thirty-five metrics were derived using ENVI 4.5 software. These metrics include maximum, minimum, mean, standard deviation (st), and coefficient of variance (cv) of the digital numbers of each lidar bin at plot level. In addition, twenty-five metrics were derived from data fusion (first five PCA components) including: maximum, minimum, mean, st, and cv of the digital numbers of each PCA component at

plot level. ENVI 4.5 software was used to derive all the metrics. Then, all the results were saved in a text file for regression analysis.

Statistical Analysis

To estimate CBD and CBH canopy fuel parameters from airborne lidar data, multiple predictive models were developed in this study. In our regression models, we used Chapter III's results (CBD_{AL}, CBD_{CM}, CBH_{LH}, and CBH_{CM}) as field data, also called reference data. Four different metric sets were used to obtain the best fitted regression models for canopy fuels and these metrics are summarized in Table 4.2: (1) a total of sixteen lidar point cloud metrics at 30 m resolution, the original eight lidar point cloud metrics and the same metrics transposed using a natural logarithmic transformation (Ln), named metrics-set-1, (2) a total of sixteen lidar point cloud metrics at actual plot size, the original eight lidar point cloud metrics and the same metrics transposed using a natural logarithmic transformation (Ln), named metrics-set-2, (3) thirty-five lidar upper bins metrics, named metrics-set-3, and (4) twenty-five data fusion PCA metrics, named metrics-set-4.

Table 4.2
Definition of metric sets used in this study.

Source	**Definition**
Metrics-set-1	sixteen lidar point cloud metrics at 30 m
Metrics-set-2	sixteen lidar point cloud metrics at actual plot size
Metrics-set-3	thirty-five lidar upper bins metrics
Metrics-set-4	twenty-five data fusion PCA metrics

Table 4.3 represents all the independent variables used in our regression analysis in this study. In this table, the subscript *i* for height bins metrics represents height bin numbers from 5 through 11 and the subscript *i* for data fusion metrics represents PCA band numbers 1 through 5, respectively. As mentioned before, log transformation was applied to all of lidar metrics. Log transformations may introduce a systematic bias into the calculations; therefore, there is a need to calculate the correction factor to neutralize this bias.

We calculated the correction factor using the following equation from Sprugel (1983):

$$Correction\ Factor = Exp(standard\ error\ of\ estimate)^2/2$$

The SPSS, Statistical Package for the Social Sciences, was used for all regression analyses in this study. As discussed in detail in Chapter III, CBD and CBH canopy fuel parameters were derived using both allometric equations and a software called CrownMass. In this chapter, results of these two methods were separately used as ground data to see which method's result has better relationship with lidar derived metrics. Stepwise regression was performed to find the best fitted model for the data at $\alpha = 0.05$ for estimating CBD and CBH from airborne lidar. The selected models were chosen based on several criteria: a good balance between a high coefficient of determination (R^2) value, a low root mean square error (RMSE), no colinearity, and parsimony, which contains a limited number of independent variables. Variance inflation tests were conducted for each selected model which is important for finding colinearity between independent variables if there is any.

Table 4.3
All the metrics used in this study to derive CBD and CBH.

Metrics	Description
Lidar point cloud metrics	
h_mean	Mean height of point cloud
h_max	Max height of point cloud
h_25	25th percentile height of point cloud
h_50	50th percentile height of point cloud
h_75	75th percentile height of point cloud
h_90	90th percentile height of point cloud
D	Density
variance(s)	coefficient of variation of point cloud
CBH_{LH}	CBH obtained from allometric equations
CBH_{CM}	CBH obtained from CrownMass program
Height Bins metrics	
Bin_i_min	Lidar Height Bin_i: Minimum DN value of plot
Bin_i_max	Lidar Height Bin_i: Maximum DN value of plot
Bin_i_mean	Lidar Height Bin_i: Mean DN value of plot
Bin_i_st	Lidar Height Bin_i: Standard Deviation DN value of plot
Bin_i_cv	Lidar Height Bin_i: Variance DN value of plot
Data Fusion metrics	
PCA_i_min	PCA $Band_i$: Minimum DN value of plot
PCA_i_max	PCA $Band_i$: Maximum DN value of plot
PCA_i_mean	PCA $Band_i$: Mean DN value of plot
PCA_i_st	PCA $Band_i$: Standard Deviation DN value of plot
PCA_i_ cv	PCA $Band_i$: Variance DN value of plot

Results and Discussion

Table 4.4 and Table 4.5 represent the selected regression models with their R^2, adjusted R^2, p-values, and RMSE values for both CBH and CBD, respectively. In these tables, $\hat{y}$ represents reference data for CBH and CBD and bias correction factors are added to the end of each predicted model.

As shown in Table 4.4, we obtained a total of eight best fitted regression models for CBH: two models from metrics-set-1 at 30 m spatial resolution; two models from metrics-set-2 at actual plot size; two best fitted models from metrics-set-3; and two best fitted models from metrics-set-4. These regression models were developed with a significant level of 0.05. All the predicted regression models provided good R^2 values, ranging from 0.662 to 0.976, and adjusted R^2 values, ranging from 0.647 to 0.973. However, only R^2 and adjusted R^2 values are not enough to select the best regression model. Therefore, all the selected models were plotted (Fig. 4.6a through Fig. 4.6h) to present the goodness-of-fit of the data to choose the best model for predicting CBH.

Overall, when comparing the CBH_{LH} and CBH_{CM} regression models for each individual metrics sets, we can see that CBH obtained from allometric equations always provided the better fitted models based on the R^2 and adjusted R^2 values with all the metric sets (1 through 4). The H_{90} was the main predictor due to its vertical location within the point cloud on all regression models obtained from lidar point cloud (metrics-set-1 and -2). Since H_{90} and CBH are related to canopy height it makes sense to have H_{90} as a main predictor. The H_{90} and D were the two main predictors obtained from metrics-set-2 at actual plot size. These results are consistent with other research that

found D and H_{90} to be a main predictor in CBH (Li et al., 2008; Erdody and Moskal, 2010; Andersen et al., 2005). In addition, LnH_{50}, LnH_{75}, $LnH_{mean,}$ and Ln_{cv} were the other predictors used on regression models obtained from Metrics-set-1 and Metrics-set-2 at both resolutions 30 m and actual plot size for estimating CBH.

As mentioned before, height bins were created by counting the occurrence of the number of lidar points within each volume unit and normalizing by the total number of points. Therefore, they are also considered as canopy density metrics. As demonstrated in earlier studies such as Popescu and Zhao (2008) and Næsset (2004), the height bins approach can be used to derive independent variable for regression models to estimate canopy characteristics. Among all the thirty-five lidar upper bins predictors, $Band6_{cv,}$ $Band7_{cv}$, $Band8_{cv,}$ and $Band9_{mean}$ were used as predictors to estimate CBH from metrics-set-3. The height values of CBH obtained from Lorey's weighted height approach varied between 0.1 m (min) and 24.3 m (max) with an average height of 10.6 m. The CBH value of a total of 24 plots is within 10 to 15 m interval (Band7), 14 plots are within 5 to 10 m interval (Band6), and 7 plot's CBH values are in 15 to 20 m interval (Band9). The coefficient of variation (cv) is the measure of dispersion of the data and also considering the total number of the plots fallen within each interval, we could expect these metrics to be included in our final fitted models.

Table 4.4
Results of the CBH regression analysis.

CBH from Metrics-set-1	Model	R^2	Adj. R^2	P-value	RMSE
CBH_{LH}: Metrics-set-1	$\hat{y} = exp(1.326 + 1.001\, LnH_{mean} - 0.036H_{50} - 1.21LnH_{90} - 1.004D + (0.195)^2/2)$	0.976	0.973	<0.0001	0.195
CBH_{CM}: Metrics-set-1	$\hat{y} = exp(3.164 + 3.118Ln(cv) - 2.21D - 2.204Ln(H_{90}) + (0.268)^2/2)$	0.945	0.942	<0.0001	0.268
CBH from Metrics-set-2					
CBH_{LH}: Metrics-set-1	$\hat{y} = exp(-1.861 + 1.805LnH_{90} - 0.044H_{max} + (0.173)^2/2)$	0.949	0.947	<0.0001	0.173
CBH_{CM}: Metrics-set-1	$\hat{y} = exp(-1.358 + 1.21LnH_{90} - 0.086LnH_{25} + (0.234)^2/2)$	0.895	0.891	<0.0001	0.234
CBH from Metrics-set-3					
CBH_{LH}: Metrics-set-2	$\hat{y} = exp\,(-0.430 + 5.537Band7_{cv} + 6.31Band9_{mean} + (0.698)^2/2)$	0.708	0.696	<0.0001	0.698
CBH_{CM}: Metrics-set-2	$\hat{y} = exp(-0.431 + 4.747Band8_{cv} + 3.818Band6_{cv} + (0.715)^2/2))$	0.662	0.647	<0.0001	0.715
CBH from Metrics-set-4					
CBH_{LH}: Metrics-set-3	$\hat{y} = exp(0.079 + 4.634PCA1_{max} + 1.82PCA3_{mean} + 1.889PCA5_{mean} + (0.464)^2/2)$	0.874	0.866	<0.0001	0.464
CBH_{CM}: Metrics-set-3	$\hat{y} = exp\,(0.048 + 4.276PCA1_{max} + 2.36PCA3_{mean} + 1.658PCA5_{mean} + (0.450)^2/2)$	0.869	0.860	<0.0001	0.450

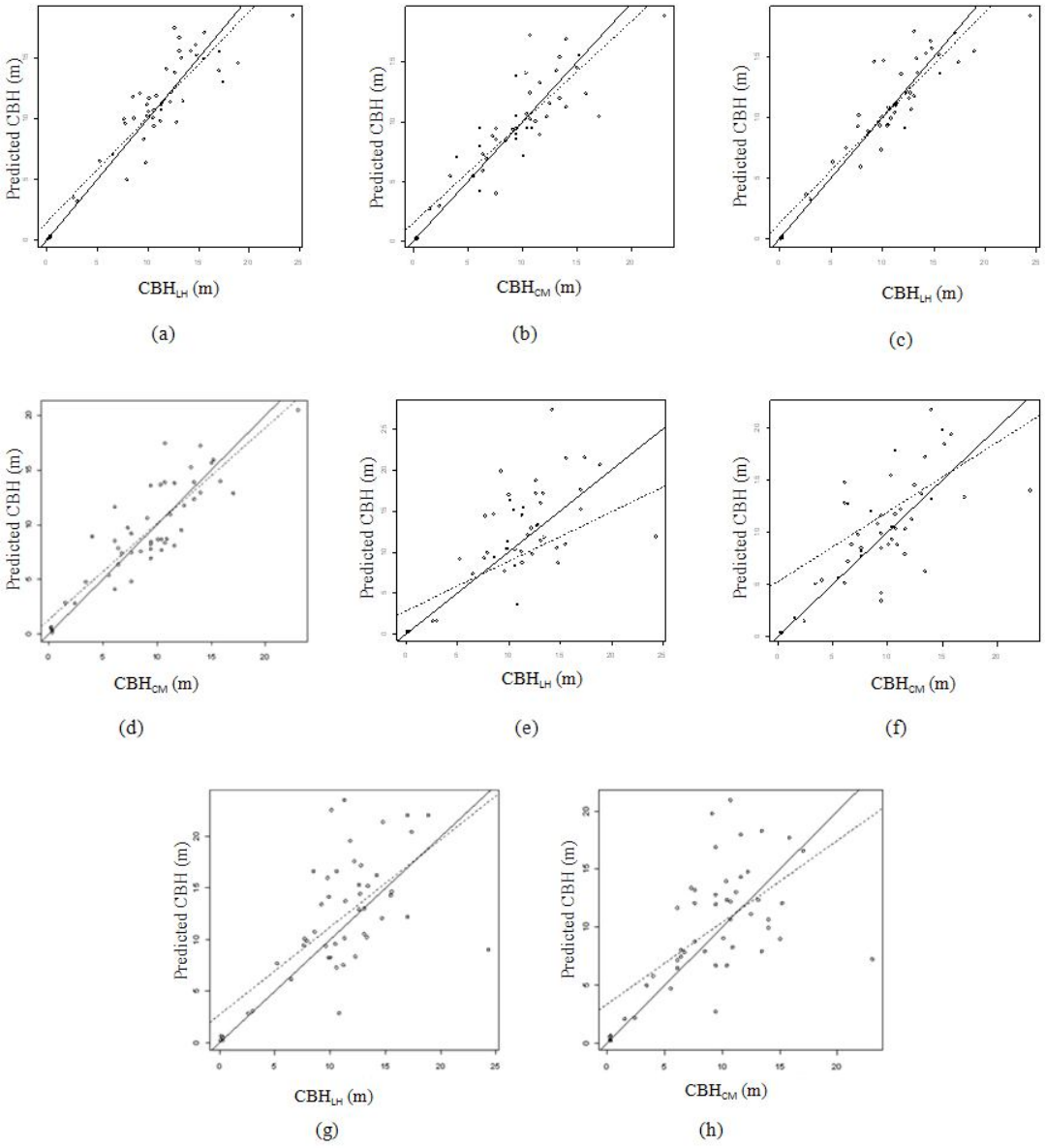

Fig. 4.6. Scatterplots of predicted CBH vs. (a) CBH_{LH} at 30 m resolution; (b) CBH_{CM} at 30 m resolution; (c) CBH_{LH} at actual plot size; (d) CBH_{CM} at actual plot size; (e) CBH_{LH} from Metrics-set-3; (f) CBH_{CM} from Metrics-set-3; (g) CBH_{LH} from Metrics-set-4; (h) CBH_{CM} from Metrics-set-4. In all figures, the solid line represents X=Y and the dashed line represents the data fit.

Among all the twenty five PCA predictors, $PCA1_{max}$, $PCA3_{mean}$, and $PCA5_{mean}$ were the key metrics used in the final fitted regression models for estimating CBH from all the metrics-set-4. The PCA considers the total variance in the data. We also calculated factor loadings for each band and PCs to see which band was used to explain the most variance in the data. The term factor loading in PCA is the simple relationship between the factors and the variables. Overall, upper lidar height bins explained the most of the variance in all PCs. The strongest relationship for PC1 was for height bins 9 (20.0-25.0 m) and 11 (>30.0 m) (6.35837 and 0.37327, respectively; Table 4.5). The PC3 has high factor loadings in lidar height bins 6 (5.0-10.0 m) and 9 (20.0-25.0 m), 0.61003 and 0.40377, respectively. The majority of the variance of PC5 was explained by lidar height bins 3 and 8 with factor loadings of 0.12811 and 0.29246, respectively. Other bands provide no useful information, contain most of the systematic noise, and/or account for very little of the variance.

Table 4.5
Result of calculated factor loadings for each PC.

Factor Loadings	Description	PC1	PC2	PC3	PC4	PC5
Quickbird Band1	Red Band	-0.45396	-0.63517	0.10342	-0.34847	-0.11252
Quickbird Band2	Green Band	0.00467	-0.00476	0.17263	-0.00696	-0.16320
Quickbird Band3	Blue Band	-0.01998	-0.01860	-0.00182	-0.01437	-0.04252
Quickbird Band4	Near Infrared Band	-0.01078	-0.00986	0.19619	-0.01460	-0.14424
Height Bin 1	0-0.5 m	0.03880	0.04041	-0.00739	0.02922	0.07593
Height Bin 2	0.5-1.0 m	-0.00330	-0.00384	0.01464	-0.00296	-0.01087
Height Bin 3	1.0-1.5 m	0.05130	0.06147	-1.40264	0.04494	0.12811
Height Bin 4	1.5-2.0 m	-0.02716	-0.03630	-0.37254	-0.02838	-0.15901
Height Bin 5	2.0-5.0 m	0.00792	0.01164	-0.76090	0.00869	0.03499
Height Bin 6	5.0-10.0 m	-0.09292	-0.11848	0.61003	-0.08721	-0.30075
Height Bin 7	10.0-15.0 m	-0.18584	-0.23506	-0.25027	-0.17176	-0.56093
Height Bin 8	15.0-20.0 m	-0.66692	-0.73436	0.15531	-0.47068	0.29246
Height Bin 9	20.0-25.0 m	0.37327	0.41207	0.40377	0.23486	-0.19930
Height Bin 10	25.0-30.0 m	-1.19969	1.45964	-0.00833	-0.86276	0.02220
Height Bin 11	>30.0 m	6.35837	0.00306	-0.01332	-1.42185	0.08858

As shown in Table 4.6, we also obtained a total of eight regression models, developed with a significant level of 0.05, for CBD canopy fuel parameter. These models were constructed using the same metrics-sets and spatial resolutions as the regression models for CBH. The estimated CBH obtained in this chapter was included as an additional variable. Bias correction factors are added to the end of each predicted model and $\hat{y}$ represents ground validation data for CBD in Table 4.6. We compared the regression models obtained from the same metrics for CBD_{AL} and CBD_{CM} to see which method's result worked the best with lidar metrics. We obtained a total of four models from lidar point cloud metrics, metrics-set-1 and metrics-set-2, and the highest R^2 and adjusted R^2 values were gathered from CBD_{AL}- Metrics-set-2 with 0.689 and 0.674, respectively, with 0.303 RMSE. The lowest R^2 and adjusted R^2 values were obtained from CBD_{CM}- at 30 m resolution with 0.473 and 0.450, respectively, with 0.554 RMSE.

For CBD from Metrics-set-3 (Table 4.6), the best R^2 and adjusted R^2 values were obtained from CBD_{AL} when used as field data with 0.748 and 0.726, respectively. For CBD from Metrics-set-4 (Table 4.6), the highest R^2 and adjusted R^2 values were obtained from CBD_{AL} with 0.700 and 0.673, respectively. As a result, CBD_{AL} used as field data always provided better models in each metrics set. To illustrate the goodness-of-fit of the data and select the best fitted model for predicting CBD, all regression models were plotted (Fig. 4.7a through Fig. 4.7h). Overall, the best fitted model based on the scatterplots, p-values, R^2, and adjusted R^2 values was obtained from Metrics-set-3 to estimate CBD canopy fuels in this study.

Some of the results in our selected regression models need to be highlighted (Table 4.6). For instance, the R^2 value obtained with CBD_{AL} was 0.748 while it was 0.403 with CBD_{CM} (Table 4.6) in the regression models obtained from Metrics-set-2. Also, the scatterplots of these two models, Fig. 4.7e and Fig. 4.7f, are quite different. In addition, the $lnCBH$ was the key predictor for estimating CBD canopy fuel parameters from CBD_{AL} in all the regression models.

Among all the best fitted regression models obtained from all metrics sets, LnCBH was the key predictor when CBD_{AL} used as reference data. Since CBD and CBH are correlated, using CBH as a predictor is adding significant explanatory power to CBD. The H_{max} was the main predictor due to its vertical location within the point cloud on all regression models obtained from lidar point cloud (metrics-set-1 and -2). These results are also consistent with other research that found $H_{90,}$ H_{mean}, and $H_{max\ to}$ be one of the predictors in CBH models (Erdody and Moskal, 2010; Andersen et al., 2005).

As expected, the LnCBH, and upper lidar height bins ($Band7_{max,}$ $Band8_{cv}$, and $Band10_{cv,}$) were used to predict CBD canopy fuel parameters in the final fitted regression models obtained from metrics-set-3. As mentioned before, studies have shown that lidar height bins approach can be used to derive independent variable for regression models to estimate canopy characteristics. Lidar height bins (Band6 and Band7) were used in the selected fitted model obtained from metrics-set-3. This model provides poor R^2 and adjusted R^2 values, 0.403 and 0.378.

Table 4.6
Results of the CBD regression analysis.

30 m resolution	Model	R^2	Adj. R^2	P-value	RMSE
CBD_{AL}: Metrics-set-1	$\hat{y} = \exp(-2.058 - 0.059H_{max} + 0.658\text{Ln}(CBH) + (0.366)^2/2)$	0.660	0.645	<0.0001	0.366
CBD_{CM}: Metrics-set-1	$\hat{y} = \exp(-1.118 - 2.927D - 0.04H_{max} + (0.554)^2/2)$	0.473	0.450	<0.0001	0.554
20 m resolution					
CBD_{AL}: Metrics-set-1	$\hat{y} = \exp(-2.139 - 0.083H_{90} + 0.814\text{Ln}(CBH) + (0.303)^2/2)$	0.689	0.674	<0.0001	0.303
CBD_{CM} : Metrics-set-1	$\hat{y} = \exp(-3.389 - 0.088H_{max} + 1.209\text{Ln}(H_{mean}) + (0.386)^2/2)$	0.647	0.630	<0.0001	0.386
CBD from Metrics-set-2					
CBD_{AL}: Metrics-set-2	$\hat{y} = \exp(-2.558 + 0.585\text{Band7}_{max} + 0.414\text{Ln}(CBH) - 1.37\text{Band10}_{cv} - 1.003\text{Band8}_{cv} + (0.329)^2/2)$	0.748	0.726	<0.0001	0.329
CBD_{CM} : Metrics-set-2	$\hat{y} = \exp(-3.733 + 1.492\text{Band7}_{max} + 1.593\text{Band6}_{mean} + (0.589)^2/2)$	0.403	0.378	<0.0001	0.589
CBD from Metrics-set-3					
CBD_{AL}: Metrics-set-3	$\hat{y} = \exp(-2.917 + 1.982\text{PCA2}_{cv} + 1.173\text{PCA2}_{min} + 2.179\text{PCA4}_{mean} + 0.285\text{Ln}(CBH) + (0.359)^2/2)$	0.700	0.673	<0.0001	0.359
CBD_{CM} : Metrics-set-3	$\hat{y} = \exp(-2.986 + 1.145\text{PCA1}_{mean} - 5.414\text{PCA5}_{st} + 1.561\text{PCA1}_{max} + (0.516)^2/2)$	0.552	0.523	<0.0001	0.516

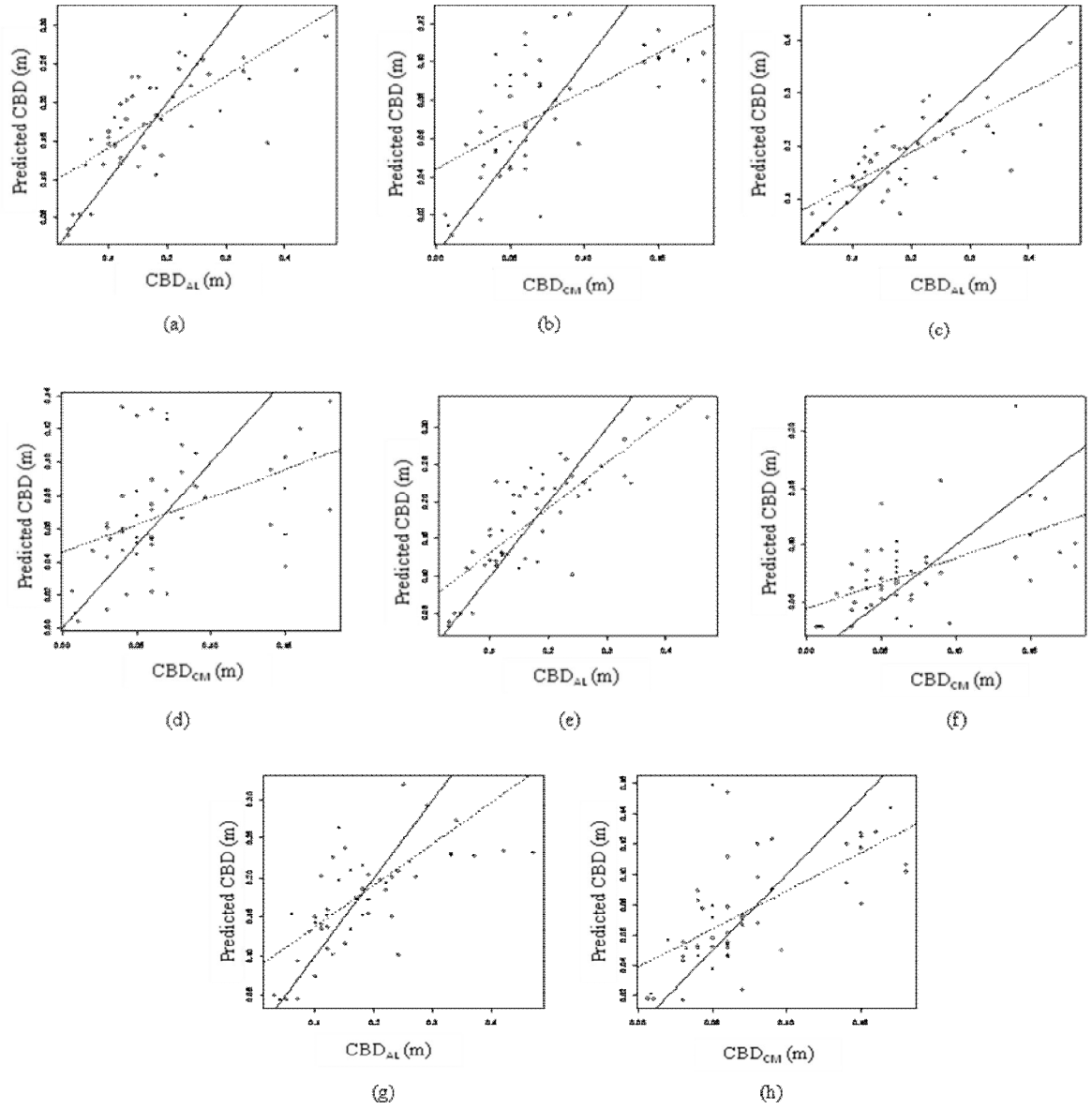

Fig. 4.7. Scatterplots of predicted CBD vs. (a) CBD_{AL} at 30 m resolution; (b) CBD_{CM} at 30 m resolution; (c) CBD_{AL} at actual plot level; (d) CBD_{CM} at actual plot level; (e) CBD_{AL} from Metrics-set-3; (f) CBD_{CM} from Metrics-set-3; (g) CBD_{AL} from Metrics-set-4; (h) CBD_{CM} from Metrics-set-4. In all figures, the solid line represents X=Y and the dashed line represent the data fit.

Among all the twenty five PCA predictors, $PCA2_{cv,}$ $PCA2_{min}$, $PCA4_{mean}$, and LnCBH were the key metrics used in the final fitted regression model for estimating CBH. In this model, CBH_{LH} was used as reference data. The PCA1 and PCA5 were the main predictors in the final model when CBD_{CM} used as reference data. As shown in Table 4.5, the upper lidar height bins were able to explain the most of the variance in both PC2 and PC5.

We derived CBD and CBH from airborne lidar data at plot level for 41 plots. The variables needed to estimate CBD and CBH were obtained from TreeVaW measurements. The estimated CBD and CBH canopy fuel parameters from TreeVaW were compared with both estimated CBD and CBH from allometric equations and CrownMass software, respectively, to see the relationship between each pair. The scatter plots of predicted CBD from TreeVaw (CBD_TreeVaw) versus CBD_{AL} and CBD_{CM} were shown in Fig. 4.8a and 4.8b. The scatterplots of predicted CBH from TreeVaw (CBH_TreeVaw) versus CBH_{LH} and CBH_{CM} were shown in Fig. 4.8c and 4.8d. These scatterplots are results of visual correlation analysis, rather than a regression analysis. Both scatterplots obtained for CBD comparison do not show strong relationship. However, the CBD_TreeVaw and CBD_{AL} demonstrated better relationship than the scatterplot of CBD_TreeVaw and CBD_{CM}. One possible explanation could be that most of the times TreeVaw captured less number of trees on each plot which might affect the result of CBD. There is a positive relationship between CBH_TreeVaw and CBH_{LH}. Since we have uniform stands in our study area and we used weighted mean

height approach to estimate CBH, the number of trees will most likely not affect the results.

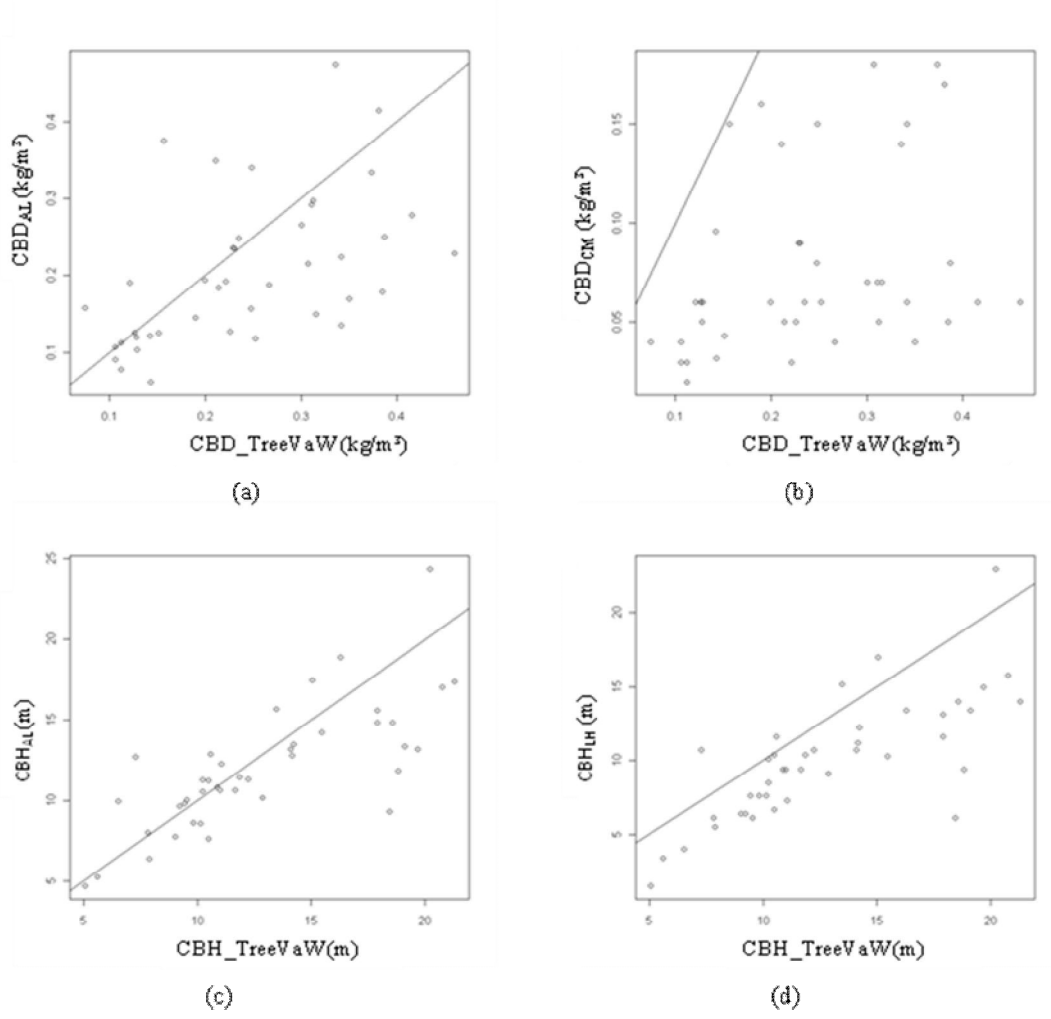

Fig. 4.8. (a) CBD_{AL} versus predicted CBD from TreeVaw, (b) CBD_{CM} software versus predicted CBD from TreeVaw, (c) CBH_{LH} versus predicted CBH from TreeVaw, (d) CBH_{CM} software versus predicted CBH from TreeVaw.

After regression models have been developed to establish a functional relationship between the airborne lidar data and the canopy fuels, CBD and CBH, the best fitted equations were used to generate maps of CBD and CBH over the entire study

area. For CBH, among all the models, the best-fitted equation was obtained from metrics-set-1 with R^2 value of 0.976 and adjusted R^2 value of 0.973. For CBD, the best fitted equation was obtained from metrics-set-3 with R^2 value of 0.748 and adjusted R^2 value of 0.726. The highest R^2 and adjusted R^2 values were used to identify the best fitted model for CBD and CBH, not the lowest log-transformed RMSE. The CBD (Fig. 4.9a) and CBH (Fig. 4.9b) maps were generated in ENVI using Band Math function based on the selected regression models.

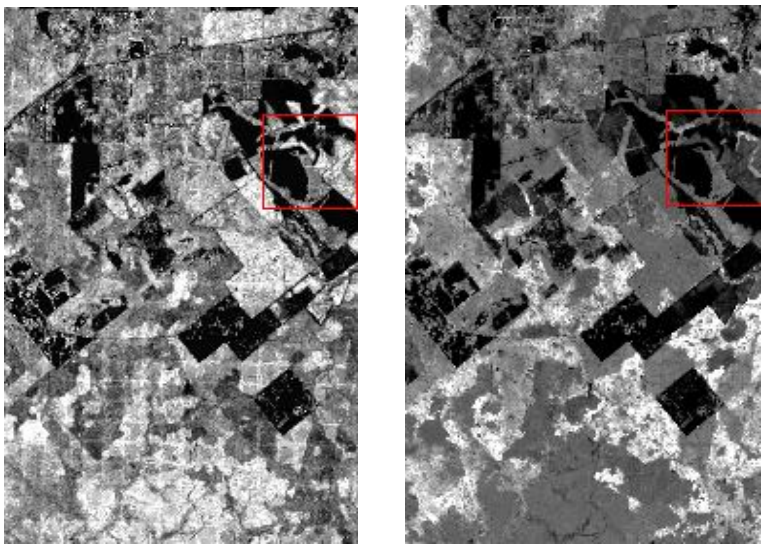

(a) (b)

Fig. 4.9. (a) The CBD map; (b) The CBH map of our study area.

Using airborne lidar data, we were able to derive the two required CBH and CBD canopy fuel parameters to simulate crown fires in FARSITE. Surface fuel model, CBD, and CBH maps are very difficult to derive and many fire managers do not have these inputs to run FARSITE. We developed all the spatial data layers for our study area. To simulate crown fire over the study area, a plot (Liv#21) was selected and plot center location was used as an ignition point in FARSITE simulations. Inside of this plot boundary, we have a total of 57 trees with an average total tree height of 52.1 m. The duration of this simulation was set to 48 hours beginning at 8:00 AM and ending at 8:00 AM two days later. Weather and wind data, gathered on March 1, 2004, were used for all runs of FARSITE because dryer periods occur during September – October and February – March in the study area. Fig. 4.10 represents the snapshot of FARSITE run. The result of FARSITE simulation shows that the estimated burned area was 463 ha (1144.57 ac) and the perimeter was 12.6 km (7.8 miles) for the selected plot (Liv#21). These results are important because a significant risk to life and property exists wherever forest stands are prone to crown fire.

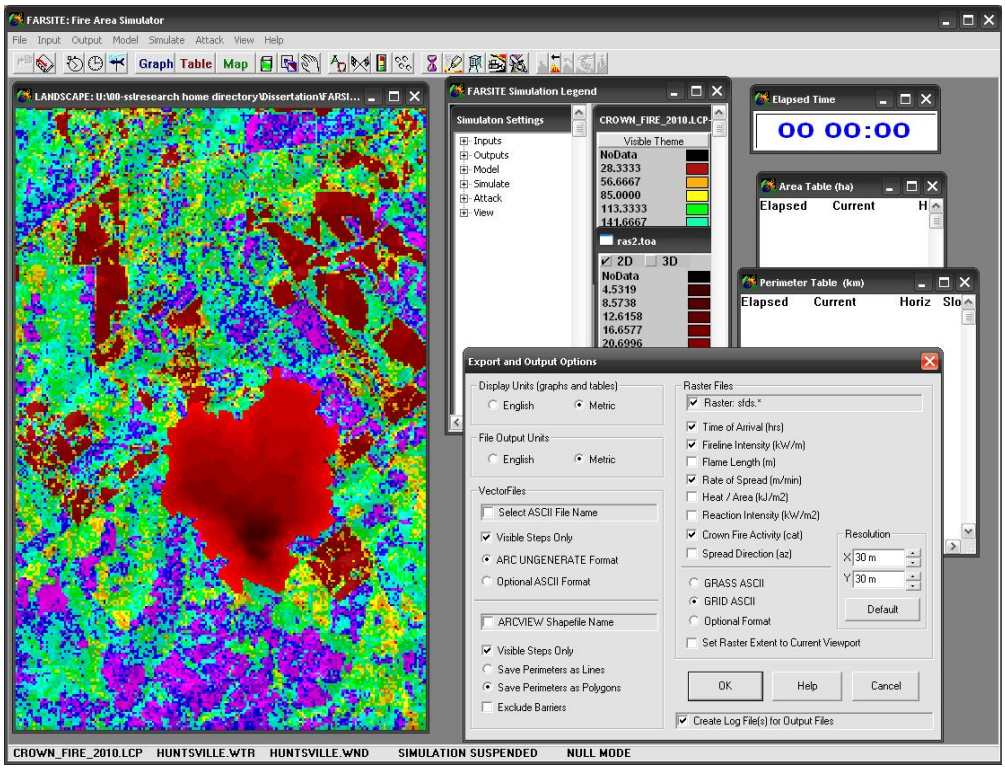

Fig. 4.10. A snapshot from crown fire simulation software, FARSITE.

Conclusions

The CBD and CBH are necessary inputs for crown fire simulation models FARSITE and others such as NEXUS. In practice, CBD has never been directly measured in the field. The CBD is the most important canopy fuel parameter because active crown fires burn the entire surface-canopy fuel complex (Cruz et al., 2003; Lefsky et al., 2001). The overall aim of this study was to estimate the two critical forest canopy parameters including CBH and CBD using airborne lidar data at plot level for loblolly pine trees in east Texas. We also aimed to map CBD and CBH from airborne lidar data and to predict the spread of wildfires using estimated forest canopy parameters as inputs into FARSITE software. The results of this study indicate that airborne lidar can be

used to generate accurate estimates of canopy fuel parameters efficiently over extensive areas of forests as demonstrated for the study area in Huntsville, TX.

The CBH and CBD cannot be directly derived from the field data because the work required to estimate these quantities across extensive areas would be problematic. Also, it is not economically and timely feasible to collect data over the large forested areas. Therefore, estimation of CBH and CBD canopy fuel parameters are based on statistical approaches using statistical metrics such as different height percentiles, mean and max height values derived from airborne lidar data for each plot. The CBH and CBD canopy fuel parameters were derived from different metrics sets in this study. The first two sets includes sixteen metrics derived from the lidar point cloud, the third metric set includes thirty-five variables from upper lidar height bins, and the last metrics set has twenty-five variables from the data fusion, stack of lidar height bins and multispectral imagery. Different resolutions were used to derive metrics from lidar point cloud (metrics-set-1). We were expecting that results at 30 m resolution would provide better models for both CBH and CBD since we have more lidar points within that grid cell size. We obtained expected results for CBH; but, the differences in the final models were not significant. However, results for CBD were unexpected and we obtained better regression models at actual plot size compared to 30 m resolution.

Among all the models, the best fitted regression model to derive CBD was obtained from metrics-set-3 based on the coefficient of determination, 0.748. In this model, CBD_{AL} results were used as ground validation data. Metrics-set-3 includes metrics derived only from lidar height bins. One of the advantages of using lidar height

bins approach is that instead of processing individual lidar points and generating metrics for these point clouds, multiple bands of lidar data are easier to process and analyze and easier to derive metrics necessary for regression analysis (Popescu and Zhao, 2008). The lidar height bins approach has high potential for becoming a standardized method for deriving CBH and CBD canopy fuel parameters. Metrics-set-2 and -3 did not improve our final models for CBH. In addition, unlike the studies of McCombs et al. (2003), Mutlu et al. (2008a), Popescu and Wynne (2004), Erdody and Moskal (2010), Varga and Asner (2008), Donoghue and Watt (2006), data fusion approach (metrics-set-3) did not provide the best estimation of canopy fuel parameters for this study.

Andersen et al. (2005) and Scott and Reinhardth (2001) used Fire and Fuels Extension to the Forest Vegetation Simulator (FFE-FVS) to derive CBH and CBD canopy fuels and then tried to derive these two metrics from airborne lidar data. In our study, we used both allometric equations and CrownMass software to derive CBH and CBD, then used both results as ground validation data when estimating these variables from airborne lidar data. Overall, CBD_{AL} and CBH_{LH} when used as ground validation data always produced better estimation of CBD and CBH compared to CBD_{CM} and CBH_{CM}, respectively. In Chapter III, we found that CBD values obtained from allometric equations are an average 2.5 times larger than CBD results obtained from CrownMass software. We also found that CBH results obtained from Lorey's Mean Height approach was 1.2 times higher than those from CrownMass software. Because of statistical errors due to equation selection, estimating coefficients, data processing errors, CBD and CBH estimated either from software and/or allometric methods, errors

are potentially introduced no matter what the scale is. As mentioned in Chapter III, it is difficult to conclude that one method is better than other. However, the results presented in this chapter demonstrated that the calculated canopy fuel parameters using airborne lidar variables coupled with allometric equations resulted in better estimation compared with those obtained from CrownMass software.

Studies have shown that CBH and CBD can be derived from allometric equations, software (e.g., FuelCalc, CrownMass, FFE-FVS), and/or airborne lidar data (Riano et al., 2003; Popescu and Zhao, 2008; Erdody and Moskal, 2010; Cruz et al., 2004; Riano et al, 2004; Hall and Burke, 2006; Keane et al., 2005; Rollins and Frame, 2006; Scott and Reinhardt, 2001; Beukema et al, 1997; Morsdof et al., 2003; Keane et al., 1998). None of the studies I have found run FARSITE to simulate crown fire behavior for their study area. There are two major reasons for that: (1) if they used allometric equations to derive CBH and CBD canopy fuels, they were not able to generate the spatial maps, (2) even if they used remotely sensed data to derive CBH and CBD and generated spatial maps, they did not have a surface fuel model map that is the other required input to run FARSITE. We employ a unique approach to derive all the required spatial data layers from airborne LIDAR and to use these data layers into FARSITE to simulate crown fire behavior over our study area, Huntsville, TX. Since crown fire data inputs are difficult to create it is presented as "optional" in the FARSITE software. Many fire managers do not have these important data layers and they are required to use very coarse estimates of these inputs. There has been no reliable, accurate, and simple method for estimating these parameters and providing high quality

inputs for FARSITE crown fire modeling. The same problem exists with other fire simulation softwares such as BehavePlus and FlamMap.

Compared to other types of fires, crown fires are relatively rare, but their impact is severe. For fire mitigation purpose, it is crucial to know both fire perimeters and fire growth areas. Fire growth area results are helpful to determine the cost of the fire. Fire perimeter results are important because they help in determining an optimal mix of fire fighting resources needed to fight fires such as dozer, tractor, crews, helicopter, engines, hourly cost of operating the resources, arrival time etc.

The advance of remote sensing technology provides a unique opportunity for alternative solutions of the forest fire problems. Applications of remote sensing to forest fire related research have been rapidly increasing in recent years. This technology can be used to decrease fire risk and to reduce fire damage. Modeling crown fire behaviors are essential for fire management activities due to the vast natural resource damage they cause, the cost of property loss, large suppression efforts, and risks to human safety. Accurate estimation of fire growth area and the direction of fire growth is critically important information for the fire management process. Knowing this essential information will avoid any health risk for local people living in the vicinity of forests with fire risk. The results of this research will provide a better understanding of enhanced fire suppression efforts, increased safety for fire crews, and will ultimately reduce threats to human safety as well as reduce the costs associated with wildfires and their suppression.

CHAPTER V

ASSESSING CANOPY FUEL PARAMETERS FROM ICESat/GLAS LIDAR DATA

Introduction

Remote sensing technologies have been used for mapping the spatial distribution of canopy and characterization of vegetation (Popescu and Zhao, 2008). Advance high resolution satellite imagery (i.e. Quickbird image) can be used to derive forest inventory data. Lidar remote sensing is a maturing and expanding technology (Hall et al., 2005; Nelson et al., 2009; Lefsky et al., 2005). Given the rapid and continuous development of lidar technology, it is expected that lidar applications in forestry will continue to rapidly increase and will become more assessable in the future. As is discussed in Chapter IV, airborne lidar data have been used for quantifying forest structures and improving management decisions. Even though airborne lidar is gaining popularity as a tool for natural resource management and datasets are becoming increasingly available (Hudak et al., 2006) and less expensive than in the past, they are still considered a costly acquisition. In addition, airborne lidar data is generally used for local and/or regional scales and rarely used for state extent level in the USA (Popescu et al., (in review); Nelson et al., 2003).

There is great interest in the potential for using Geoscience Laser Altimeter System (GLAS) on the Ice, Cloud and land Elevation (ICESat) satellite (launched on January 12, 2003) data in forest inventories in recent years (Zwally et al., 2002; Sun et al., 2008; Popescu et al., in (review); Ranson et al., 2004; Lefsky et al., 2005).

ICESat/GLAS is a large footprint full waveform satellite data. It is also the first spaceborne lidar tool that can be used to obtain continued global observation of the Earth (Simard, et al., 2008; Pang et al., 2008; Nelson et al., 2009). Mainly, it was designed to measure and monitor ice sheet mass balance, cloud and aerosol heights, and surface elevation changes (Zwally et al., 2002; Sun et al., 2008; Nelson et al., 2009; Simard et al., 2008). This system provides data for global scales and the data were obtained for over 250 million individual lidar observations. In addition, ICESat-II, future National Aeronautics and Space Administration (NASA) mission, is the 2nd generation of the orbiting laser altimeter. It is planned to launch in late 2015 (Abdalati et al., 2010). Measuring the ice sheet changes, sea ice thickness, vegetation biomass, and vegetation canopy heights are the main objectives of ICESat-II (Abdalati et al., 2010). The footprint size will be approximately 50 m at 50 Hz pulse repetition frequency, which will provide 20% more dense sampling than that of ICESat. The space between the footprints will be 140 m along-track (Abdalati et al., 2010). However, this mission is still in the early development stage; therefore, technical specifications of this upcoming mission are subject to change.

The ICESat system records the reflected energy from the ground surface as a function of time by sending the laser pulses with 40 Hz frequency and 5 ns duration and recording the returned laser pulses as a vertical profile within footprint (Sun et al., 2008; Popescu et al., (in review); Pang et al., 2008; Nelson et al., 2009). There are three spaceborne ICESat/GLAS lasers onboard: LASER 1 (L1), LASER 2 (L2), and LASER 3(L3) and operated one at a time (http://nsidc.org/data/icesat/laser_op_periods.html).

The ICESat has been in an orbit that repeats ground tracks every 91 days and each data acquisition period has ~33 days of data (Sun et al., 2008).

The GLAS waveform data has close correlation with aboveground biomass and canopy height that are measured on ground plots in extensive forests (Boudreau et al., 2008; Sun et al., 2008); therefore, it has been used for forestry studies in recent years. Lefsky et al. (2005) combined ICESat/GLAS waveforms and ancillary topography from SRTM to obtain maximum forest height in three different ecosystems located in Brazil, Tennesse, and Oregon, USA. Sun et al. (2008) used GLAS data to derive vertical structure of forests in Maryland, USA and compared their results with LVIS data (Laser Vegetation Imaging Sensor). Nelson et al. (2009) used GLAS and MODIS (MODerate resolution Imaging Spectrometer) data to estimate forest timber volume in Siberia. Simard et al. (2008) focused on how to use ICESat/GLAS to estimate the extent, height, and biomass of the mangrove forests in Colombia. This system has potential for deriving forest canopy structure.

There are three general alternative approaches for obtaining forest canopy fuel parameters: (1) field measurements, which are also needed for testing and validating all remote sensing methods, (2) statistical models, and (3) remotely sensed data including multispectral images (i.e. Quickbird, Digital Orthophoto Quarter Quad (DOQQ), or SPOT), airborne lidar, and spaceborne ICESat/GLAS lidar data. The overall objective of this chapter is to investigate the use of spaceborne ICEsat /GLAS lidar data for characterizing canopy fuel parameters in east Texas.

The total vegetation height, vertical canopy structure, and aboveground biomass were derived from ICESat/GLAS; however, the CBH has never been derived from satellite ICESat/GLAS data before. Also, our research is unique in that we investigate the utility of spaceborn GLAS waveform data to estimate CBH canopy fuel parameter using a wall-to-wall airborne lidar-derived CBH map, as reference data.

Materials and Methods

Data

Two types of data were used in this study: airborne LIDAR and spaceborne ICESat/GLAS data. Because no coincident field measurements are directly available over the footprints of GLAS shots, a two-phase approach were used in developing the regression models. First, a spatially-explicit map of CBH was derived from airborne lidar data. Then, the GLAS metrics were related to this lidar-derived canopy characteristic with multiple linear regression models. The CBH was obtained from both the field data (Chapter III) and the airborne lidar data (Chapter IV). The details of airborne data and study area were discussed in Chapter IV.

Spaceborne ICESat/GLAS data

We were able to obtain GLAS data for our study area from February 2004 to October 2007 with GLAS sub-cycles from L2A to L3I from http://www.nsidc.org/data/icesat/order.html. Among all of the available GLAS data, we used the February 2004 GLAS data set obtained from GLAS L2B sub-cycle. This set of

GLAS data was collected during the leaf-off season, the same time period the airborne lidar data was collected. As mentioned in studies of Boudreau et al. (2008) and Popescu et al. (in review), data obtained from different season might create high variation in our regression analysis and increase the temporal inconsistency between airborne lidar and GLAS data. Sun et al. (2008), Duong et al. (2006), Boudreau et al. (2008), and Ashworth et al. (2010) compared their estimations of canopy heights from different observation periods of ICESat GLAS data to analyze the season and timing effects on their estimations. They found that GLAS data obtained from different time periods contain different amount of signals, which affect estimation of variables such as biomass and canopy heights. Therefore, we only used February 2004 GLAS dataset to match with airborne lidar data information to avoid any problems.

The GLA01 and GLA14 were the two primary GLAS data that we used in this study. The GLA01 (level 1) data provides waveforms for each laser shots (Sun et al., 2008; Boudreau et al., 2008). Energy returned from the surface is recorded into 1000 samples at two different sampling intervals, 5 ns or 1 ns, with sampling the last 544 bins at 1 ns (equal to 15 cm) (Neuenschwander et al., 2008). The land surface altimetry GLA14 (level 2) data provides canopy/ground elevations and laser range information for signal beginning and end, the location, and width of the six Gaussian peaks that provides the shape of waveforms (Sun et al., 2008; Nelson et al., 2009).

This spaceborn lidar system emits 40 pulses per second with a footprint of 65 m nominal diameter. The diameter of the footprints changed for each laser (Neuenschwander et al., 2008). The space between each footprint was 172 m apart along

track (Zwally et al., 2002; Nelson et al., 2009). In the waveform data, the first signal represents the maximum height and the last signal represents the ground data (Zwally et al., 2002; Nelson et al., 2009; Popescu et al., (in review); Sun et al., 2008). A total of 48 GLAS waveforms were found and overlaid on our entire study area. Fig. 5.1 represents the overall view of the ICESat/GLAS footprints over lidar-derived CBH map of the study area.

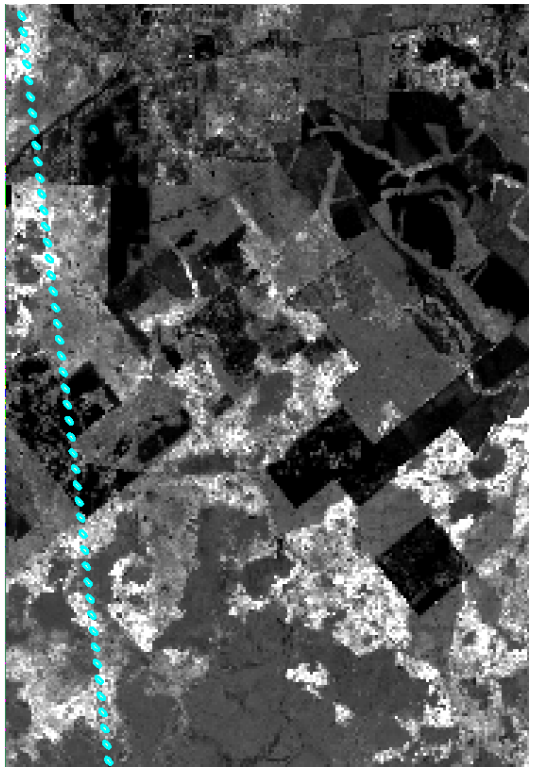

Fig. 5.1. The ICESat/GLAS footprints overlaid on the airborne lidar-derived wall-to-wall CBH map of our study area.

Processing ICESat/GLAS Waveform Data

Initially, a total of 48 GLAS waveforms were found and overlaid over the study area; however, only the 33 of the GLAS waveforms were used because no information was obtained from the rest of the footprints. The GLAS metrics obtained from Popescu et al. (in review) were used in this study to derive the CBH canopy fuel parameter. After ordering and downloading the GLAS data from the NSIDC (National Snow and Ice Data Center) website for our study area, the GLAS data were processed as described in Popescu et al. (in review). A standalone peak finding algorithm developed by Neuenschwander et al. (2008) was used to process the GLAS waveform data. Similar to studies of Nelson et al. (2009), Neuenschwander et al. (2008), Sun et al. (2008), and Boudreau et al. (2008), each waveform was extracted and processed to derive energy quartile heights (also called GLAS metrics) for our study area.

The GLA14 provides the latitude and longitude information. With the information obtained from GLA14, the last 392 records of each GLAS waveform (GLA01) were geolocated. The vegetation height and ground height were derived using GLA14 product. On vegetated areas, the laser pulses interact with a complex surface; therefore, the returned waveform is modeled as a mixture of Gaussian (Neuenschwander et al., 2008). By applying the Gaussian filters, GLAS waveforms were smoothed using Gaussian peaks at different heights. The ground was determined using the elevation information at the maximum location on the last Gaussian peak. The GLAS waveform extent is obtained by computing the differences between the signal beginning and ending. The tree top information was obtained by computing the distance between the

signal beginning and the signal ending, which is the last Gaussian peak.

After obtaining total waveform energy, the position of 0% (RH0), 25% (RH25), 50% (RH50-HOME (height of median energy)), 75% (RH75), 90% (RH90), and 100% (RH100) percentile heights were computed starting from the signal ending by computing a cumulative distribution function of GLAS waveform energy. RH0 is the ground energy and RH100 represents energy at the top of canopy. The HOME was calculated by finding the median of the entire signal from the waveform; including energy returned from both canopy and ground surfaces. The location of the median energy is then referenced to the center of the last Gaussian pulse to derive a height value. By getting the ratio between ground and total waveform energy, the energy penetration index (EPI) was computed. A total of ten GLAS metrics were derived and used in our regression analysis to estimate CBH.

First, a spatially-explicit map of CBH was needed as a reference for using GLAS data to estimate the CBH canopy fuel parameter. The wall-to-wall CBH map was generated and details were given in Chapter IV. After obtaining all the GLAS waveform metrics, we needed to tie GLAS data to the wall-to-wall map of CBH obtained from airborne lidar data. Similar to studies of Neuenschwander et al. (2008) and Pang et al. (2008), the exact shape of ellipsoid GLAS footprint was used in this study. The canopy/ground elevation in GLA14 is positioned to TOPEX/Poseidon ellipsoid and the coordinates of our airborne lidar data are referenced to WGS-84. Therefore, the coordinates of GLAS waveforms were converted to WGS-84 using a conversion tool named as “Research Coordination Network Utilities and Tools” obtained from the

Montana State University and Yellowstone National Park website (http://www.rcn.montana.edu/resources/tools/coordinates.aspx). The TOPEX/Poseidon ellipsoid and WGS-84 are similar, the main difference between the two is that there is 60 cm difference in the semi-major axis (Neuenschwander et al., 2008).

The exact ellipsoid shape of each GLAS footprint was determined by using major ellipse axis, eccentricity, and azimuth orientation. The location accuracy of each GLAS footprint was evaluated by matching the elevation profile from GLAS with the airborne lidar derived elevation obtained from Popescu et al. (in review). A shapefile of these footprints was created. Then, the shapefile was converted to ROIs (region of interests) using ENVI 4.5 software and displayed over the wall-to-wall of CBH map. Using the ROI statistics tool, we extracted average CBH values within each GLAS footprint boundaries on lidar-derived CBH map and recorded them as a text file for statistical analysis. Fig. 5.2. represents an example of waveform data collected by ICESat/GLAS.

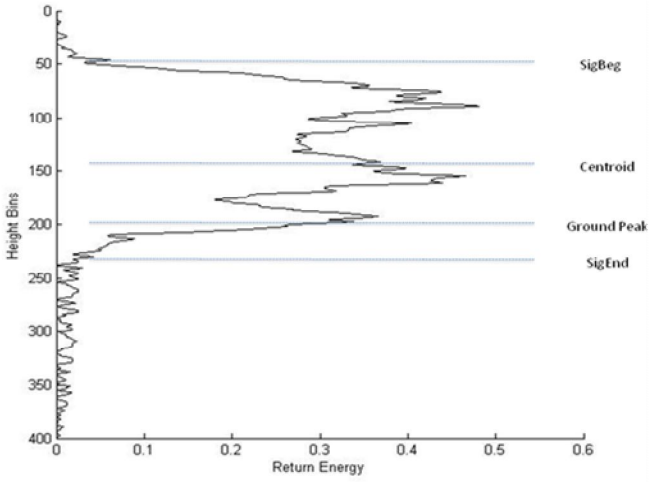

Fig. 5.2. The GLAS example waveform over forest land.

Statistical Analysis

The SPSS, Statistical Package for the Social Sciences (IBM company), was used in this study for our statistical analysis. Simple linear regression was used to derive CBH from GLAS data. The mean CBH value obtained from lidar derived CBH map on each GLAS footprint was used as dependent variable and GLAS metrics were used as independent variables in our investigations. Stepwise regression analysis was performed to find the best fitted model with a significant level of 0.05 for estimating CBH from GLAS waveform data. The best fitted model was chosen based on: a high coefficient of determination (R^2) value, a low root mean square error (RMSE), no collinearity, and a scatterplot which shows the goodness-of-fit of the data.

Results and Discussion

According to regression analysis result, GLAS height metrics and lidar-derived CBH were highly correlated in this study. Fig. 5.3 represents a comparison of average CBH at footprint level between airborne lidar and GLAS waveforms over a total of 33 leaf-off waveforms. The solid line represents X = Y and the dash line represents the data fit in Fig. 5.3. The R^2 and adjusted R^2 values of the selected best-fitted model are 0.88 and 0.876, respectively, with a low RMSE of 1.76. This correlation relates to the predictability of lidar-derived CBH from GLAS waveform data. Among all the metrics (SigBeg, SigEnd, RH25, RH90, etc.) derived from GLAS data, the main predictor in our final model is HOME metric. The result is not surprising since HOME (RH50) is proven to be a useful GLAS metric in estimating forest structural attributes at the footprint level

by several studies, such as Drake et al. (2002) and Anderson et al. (2006).

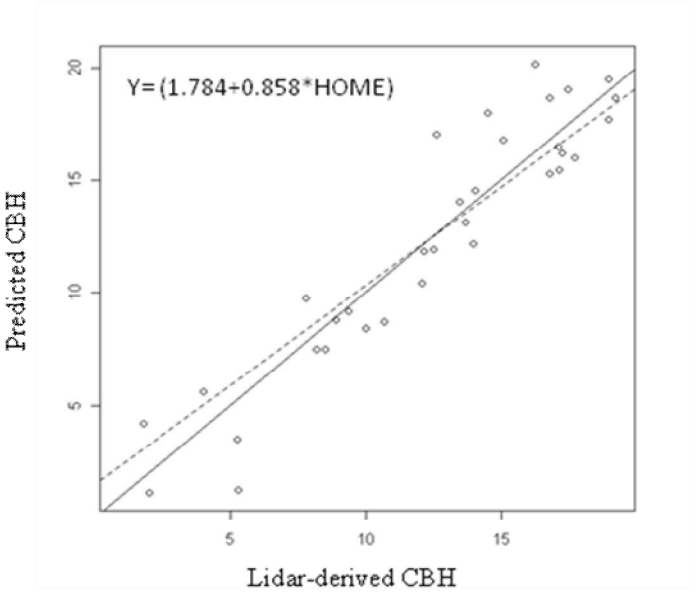

Fig. 5.3. A scatterplot of CBH from airborne lidar data vs. estimated CBH from GLAS data.

Similar to studies from Sun et al. (2008), Popescu et al. (in review), Ashworth et al. (2010), and Neuenschwander et al. (2008), we also used an average value of our dependent variable (CBH). Our findings show that the average value extracted from the lidar-derived CBH map within each GLAS footprint boundary was able to examine the utility of GLAS data for estimating CBH canopy fuel. Our initial attempt was to derive both CBH and canopy bulk density (CBD) canopy fuel parameters from GLAS data. Even though we were successful in estimating CBH, we were not successful in estimating CBD from GLAS waveform data. One possible explanation is that CBD is not a direct function of vegetation height, canopy energy, or any energy percentile because CBD is the ratio between foliage biomass and crown volume. Therefore, we

believe there is not a direct linear relationship between CBD and these GLAS metrics. Another explanation could be the use of allometric equations to derive CBD from field data. Allometric equations utilizing field measurements often produce imperfect results; the error in these results can be propagated through data processing and increase errors (Popescu et al., (in review)). In addition, the CBD map derived from airborne lidar data might also contain errors. Lastly, the algorithm written by Neuenschwander et al. (2008) may not capture necessary information from the GLAS waveform data that could affect the estimation of CBD from GLAS data.

The correlation between each energy percentile (RH75, RH90, etc.) and the lidar-derived CBH was analyzed. We found that all metrics, except for the HOME energy percentile, were poorly correlated with lidar-derived CBH. In Chapter IV, CBH is proven to be a good predictor for estimating CBD. In addition, we also obtained a good model for predicting CBH from GLAS data ($R^2 = 0.88$). We analyzed the correlation between CBD and CBH canopy fuel parameters (Fig. 5.4). In Fig. 5.4, we can see there is a negative correlation between the two parameters. Five outliers can be clearly seen on the bottom left of Fig. 5.4.

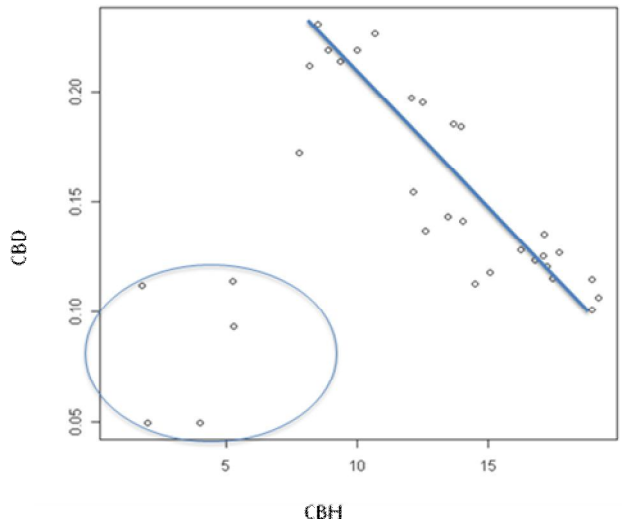

Fig. 5.4. Scatter plot of CBD and CBH.

Conclusions

In this chapter, we investigated the use of ICESat/GLAS waveform data for estimating forest canopy fuel parameters. As discussed in Chapter IV, we were successfully able to generate a wall-to-wall CBH map using airborne lidar data. In this chapter, we used Chapter IV's result as a reference to estimate canopy fuel parameters from GLAS data. We used a variety of GLAS metrics such as HOME (height of medium energy), percentile height, and energy penetration to test their usefulness to predict canopy fuel parameters through regression analysis. The only significant GLAS to estimate CBH in this study metrics was the HOME variable. We extracted CBH within the exact shape of the GLAS footprint. To derive some variables, such as biomass, other studies collected field data within the GLAS footprints. This method is time consuming and less efficient than using remotely sensed data i.e., multispectral imagery,

LVIS, or SRTM data (Ashworth et al., 2010). In this study, we used airborne lidar data and spaceborne GLAS data to estimate canopy fuel parameters. Our results indicated that GLAS waveform data can be used to accurately estimate the CBH canopy fuel parameter, but not the CBD.

CHAPTER VI

CONCLUSIONS

Canopy fuel parameters are important model inputs for fire simulation software such as FARSITE and FlamMap. Fire managers and scientists need to estimate these parameters as accurately as possible (Raccoforte et al., 2008; Scott & Reinhardth, 2001). Accurate estimation of fire growth area and the direction of fire growth is important information for the fire management process. To improve ecosystem health, there is a need to use complex fire behavior models to support environmental assessments. The overall aim of this study was to derive two important canopy fuel parameters, canopy base height (CBH) and canopy bulk density (CBD), using in-situ, airborne lidar and spaceborne GLAS data in Texas.

In Chapter III, species-specific allometric equations and the CrownMass program were used to derive CBD and CBH canopy fuel parameters. We emphasized the importance of using species-specific equations and the effect of tree crown shape on CBD calculation. In addition, using Lorey's weighted mean crown base height calculations provided promising result on CBH calculation. The results from both methods, allometric equations and the CrownMass program, were compared. Chapter III also highlighted that these two important canopy fuel parameters can be derived using allometric equations. To the best of my knowledge, this approach has never been used and there is no published study on calculating species-specific CBD for forests similar to stand conditions in East Texas. This is an important step because ground inventory data

are needed to derive canopy fuel parameters and generate maps from remote sensing data. The accuracy of these calculations and availability of these methods are very important for fire managers.

Airborne LIDAR systems can be used for fire detection, location, and mapping for burned area assessment, and, important to this study, for canopy fuel assessment and mapping (Keane et al., 1998; Mutlu et al., 2008b). Chapter III's results were used as ground inventory data in Chapter IV to validate CBD and CBH estimates from airborne lidar data. The results of Chapter IV indicate that airborne lidar can be used to efficiently generate accurate estimates of canopy fuel parameters over extensive forested areas such those presented in our study area in Huntsville, TX. We developed a methodology for assessing and mapping CBD and CBH with lidar derived metrics at multiple spatial resolutions for loblolly pine trees. The lidar point cloud, lidar height bins, and data fusion approaches were used in Chapter IV. Since canopy fuel parameters cannot be directly measured from the field data, statistical approaches were developed for using metrics such as different height percentiles and density values derived from airborne lidar data for each plot. To derive CBD, the best fitted regression model was obtained from the height bins approach lidar point cloud metrics based on the coefficient of determination, 0.748. In this model, the CBD_{AL} results were used as ground validation data. To derive CBH, the best fitted regression model was obtained from metrics-set-1 based on the coefficient of determination, 0.976.

The lidar height bins approach has high potential for becoming a standardized method for processing and exchanging forestry lidar data. The lidar bins used in this

study contain detailed information on forest canopy structure. Zhao and Popescu (2008), Mutlu et al. (2008a), Griffin et al. (2008), and Næsset (2004) also used the height bins concept for mapping surface fuels, leaf area index (LAI), percent canopy cover, vertical structure of individual tree crowns, and tree heights. In addition, Principal Component Analysis (PCA), one of the most popular and effective image fusion techniques, was also used in this study. The PCA technique has been used in studies of Zhang 2004, Fauvel et al. 2009, Mutlu et al. 2008a for urban classifications, vegetation classifications, and wetland change detection. In our analysis, the PCA technique did not provide the best result for assessing CBH and CBD canopy fuel parameters. The CBH and CBD canopy fuel maps necessary for FARSITE crown fire simulations were generated based on the selected best regression models, respectively.

Airborne and spaceborne lidar, ICESat/GLAS waveform data, were used in Chapter V. Several metrics derived from GLAS waveform data were investigated to determine their usefulness for estimating canopy fuel parameters through regression analysis. The GLAS waveform data have been proven to be useful global data for deriving forestry parameters (Popescu et al. (in review); Sun et al., 2008; Duncanson et al., 2010; Ashworth et al., 2010; Xing et al., 2010; Nelson et al., 2009). Our results indicated that GLAS waveform data can be used to accurately estimate CBH, but not the CBD fuel parameter. To the best of my knowledge, this is the first study that analyzes of the ability of satellite waveform data to assess canopy base height. Further analysis will be carried out using GLAS waveform data and multispectral image to derive surface and canopy fuel maps.

Once detailed field data are collected, the methods presented in this dissertation can be applied to any study areas located in eastern Texas. The surface fuel model map produced by Mutlu et al. (2008a) and canopy fuel maps produced by this research were used as inputs into the fire simulation software, FARSITE. We obtained burned area and perimeter information for the selected plot in our study area. For fire mitigation purposes, there is a need to know both fire perimeters and fire growth areas. Fire growth area results are important for determining the cost of a fire. Fire perimeter results are important because they help to determine the fire fighting resources needed to fight fires. Improving the accuracy of mapping canopy fuel is essential for fuel management decisions and explicit fire behavior prediction to support real-time suppression tactic and logistics decisions. Small errors in fuel parameters may not be significant for small study areas; however, for large study areas, small errors could accumulate over the duration of the fire simulation leading to large errors in predicted fire sizes. This study will assist fire managers with the mitigation of the harmful effects of wildfire. It also gives the power of sound, accurate, and efficient fire behavior modeling technology to forest fire fighters. The accurate prediction of the potential risk of a wildland fire is necessary to reduce the occurrence and seriousness of wildland fires. Our results could significantly impact forest policy and forest resource management.

REFERENCES

Abdalati, W., Zwally, H. J., Bindschadler, R., Csatho, B., Farrell, S. L., Fricker, H. A., Harding, D., Kwok, R., Lefsky, M., Markus, T., Marshak, A., Neumann, T., Palm, S., Schutz, B., Smith, B., Spinhirne, J., & Webb, C. (2010). The ICESat-2 Laser Altimetry Mission. *Proceedings of the IEEE, 98*, (5), 735-751.

Agee, J. K., Berni, B., Finney, M. A., Omi, P. N., Sapsis, D. B., Skinner, C. N., Van Wagtendonk, J. W., & Weatherspoon, C. P. (2000). The use of shaded fuel breaks in landscape fire management. *Forest Ecology and Management, 127*, 55-66.

Agee, J. K. & Skinner, C. N. (2005). Basic principles of forest fuel reduction treatments. *Forest Ecology and Management*, *211*, 83-96.

Allen, C. D., Savage, M., Falk, D. A., Suckling, K.F., Swetnam, T.W., Schulke, T., Stacey, P.B., Morgan, P., Hoffman, M., & Klingel, J.T. (2002). Ecological restoration of Southwestern ponderosa pine ecosystems: a broad perspective. *Ecological Applications, 12*, 1418-1433.

Andersen, H. E., McGaughey, R. J., & Reutebuch, S. E. (2005). Estimating forest canopy fuel parameters using lidar data. *Remote Sensing of Environment, 94*, 441-449.

Andrews, P.L. (1986). *BEHAVE: fire behavior prediction and fuel modeling system—BURN subsystem, Part 1. General Technical Report INT-194*. Ogden, UT: U.S.

Department of Agriculture, Forest Service, Intermountain Research Station 130 pp.

Andrews, P. L. & Queen, L. P. (2001). Fire modeling and information system technology. *International Journal of Wildland Fire*, *10*, 343-352.

Arroyo, L. A, Pascual, C., & Manzane, J. A. (2008). Fire models and methods to map fuel types: The role of remote sensing. *Forest Ecology and Management*, *256*, 1239-1252.

Ashworth, A., Evans, D. L., Cooke, W. H., London, A., Collins, C., & Neuenschwander, A. (2010). Predicting southeastern forest canopy heights and fire fuel models using GLAS data. *Photogrammetric Engineering and Remote Sensing, 76*, 915–922.

Avery, T. E. & Burkhart, H. E. (1983). *Forest measurements*. McGraw-Hill series in forest resources. New York: McGraw-Hill Book Company.

Baldwin, V. C. & Peterson, K. D. (1997). Predicting the crown shape of loblolly pine trees. *Canadian Journal Forest Research, 27*, 102-107.

Beukema, S. J., Greenough, D. C., Robinson, C. E., Kurtz, W. A., Reinhardt, E. D., Crookston, N. L., Brown, J. K., Hardy, C. C., & Stage A. R. (1997). An introduction to the fire and fuels extension to FVS. In R. Teck, M. Mouer, & J. Adams (Eds.), *Forest vegetation simulator: Conference proceedings. February 3-7, 1997* (pp. 191-195). Fort Collins, CO: U.S. Department of Agriculture, Forest Service, Intermountain Research Station.

Boudreau, J., Nelson, R. F., Margolis, H. A., Beaudoin, A., Guindon, L. & Kimes, D. S. (2008). Regional aboveground forest biomass using airborne and spaceborne lidar in Québec. *Remote Sensing of Environment, 112***,** 3876- 3890.

Brack, C. (1999). Lorey's mean height, forest measuring and modeling. The Australian National University. http://srs-associated.anu.edu.au/mensuration/s_height.htm (Accessed on December 7, 2009).

Brown, J. K. (1978). *Weight and density of crowns of Rocky Mountain conifers. General Technical Report INT-RP-197*. Ogden, UT: U.S. Department of Agriculture, Forest Service, Intermountain Forest and Range Experiment Station 56 pp.

Carreiras, J. M. B., Pereira, J. M. C. & Pereira, J. S. (2006). Estimation of tree canopy cover in evergreen oak woodlands using remote sensing. *Forest Ecology and Management*, *223*, 45-53.

Castro, R., & Chuvieco, E. (1998). Modeling forest fire danger from geographic information systems. *Geocarto International* ,*13*, 15–23.

Chuvieco, E. & Congalton, R. G. (1989). Application of remote sensing and geographic information systems to forest fire hazard mapping. *Remote Sensing of Environment*, *29*, 147-159.

Cohen, J. D., Finney, M. A., & Yedinak, K. M. (2006). Active spreading crown fire characteristics: Implications for modeling. *Forest Ecology and Management*, *234*, 87-95.

Cruz, M. G., Alexander, M. E., & Wakimoto, R. H. (2003). Assessing canopy fuel stratum characteristics in crown fire prone fuel types of western North America. *International Journal of Wildland Fire, 12*, 39-50.

DeBano, L. F, Neary, D. G., & Ffolliott, P. F. (1998). *Fire's effects on ecosystems*. New York: Wiley & Sons Press.

DigitalGlobe, (2010). Satellite multispectral Quickbird image. DigitalGlobe, Inc. http://www.digital globe.com/index.php/85/QuickBird. (Accessed on April 15, 2010).

Donoghue, D. N. M., & Watt, P. J. (2006). Using LiDAR to compare forest height estimates from IKONOS and Landsat ETM+ data in Sitka spruce plantation forests. *International Journal of Remote Sensing*, *27*, 2161−2175.

Drake, J., Dubayah, R., Know, R., Clark, D., & Blair, J. (2002). Sensitivity of large footprint lidar to canopy structure and biomass in a neo-tropical rainforest. *Remote Sensing of Environment*, *81*, 378-392.

Dubayah, R. O., & Drake, J. B. (2000). Lidar remote sensing for forestry applications. *Journal of Forestry, 98*, 44-46.

Duncanson, L. I., Nlemann, K. O., & Wulder, M. A. (2010). Estimating forest canopy height and terrain relief from GLAS waveform metrics. *Remote Sensing of Environment*, *114*, 138-154.

Duong, H. V., Pfeifer, N., & Lindenbergh, R. (2006). Analysis of repeated ICESat full waveform data: methodology and leaf-on / leaf- off comparison. *Proceedings of*

3D Remote Sensing in Forestry, February 2006 (pp. 30-35). Enschede, The Netherlands.

Erdody T., & Moskal, L. M. (2010). Fusion of lidar and imagery for estimating forest canopy fuels, *Remote Sensing of Environment*, *114*, 725-737.

Fahnestock, G. R. (1970). *Two keys for appraising forest fuels. General Technical Report PNW-99*. Portland, OR: U.S. Department of Agriculture, Forest Service, Pacific Northwest Forest and Range Experiment Station pp 23.

Faiella, S. M. (2005). Fire, fuel, and structural dynamics in treated and untreated ponderosa pine forests of Northern Arizona. M.S. thesis, Northern Arizona University, Flagstaff, AZ.

Falkowski, M. J., Gessler, P. E., Morgan, P., Hudak, A. T., & Smith A.M.S. (2005). Characterizing and mapping forest fire fuels using Aster imagery and gradient modeling. *Forest Ecology and Management*, *217*, 129-146.

Fauvel, M., Chanussot, J., & Benediktsson, J. A. (2009). Kernel principal component analysis for the classification of hyperspectral remote sensing data over urban areas. *Journal of Advances in Signal Processing, 10*, 14-28.

Finney, M. A. (1994). Modeling the spread and behavior of prescribed natural fires. *Proceedings of Society of American Foresters, October 1993* (pp.138-143). Bethesda, MD.

Finney, M. A. (1995). *FARSITE Fire Area Simulator. Version 1.0. User guide and technical documentation*. Missoula, MT, Systems for Environmental Management Report 47 pp.

Finney, M. A. (1998). *FARSITE: Fire Area Simulator Model development and evaluation. General Technical Report RMRS-RP-4*. Ogden, UT: U.S. Department of Agricultural, Forest Service, Rocky Mountain Research Station 55 pp.

FMAPlus3, (2003). *Fuel management analyst suite version 3. Getting started, program installation, updating and general information*. Sandy, OR: Fire Program Solutions/Acacia Services.

Fox, J. (1997). *Applied regression analysis, linear models, and related methods.* Thousand Oaks, CA: Sage Press.

Fule P. Z., Waltz A.E.M., Convington W.W., & Heinlein T.A (2001). Measuring forest restoration effectiveness in reducing hazardous fuels. *Journal of Forestry, 11*, 24-29.

Griffin, A. M. R., Popescu, S. C., & Zhao, K. (2008). Using lidar and normalized difference vegetation index to remotely determine LAI and % canopy cover. *Proceedings of Silvilaser,* September 2008 (pp. 446-455). Edinburgh, UK.

Hall, S. A., & Burke, I C. (2006). Considerations for characterizing fuels as inputs for fire behavior models. *Forest Ecology and Management, 227*, 102-114.

Hall, S. A., Burke, I. C., Box, D. O., Kaufmann, M.R., & Stoker, J. M. (2005). Estimating stand structure using discrete-return lidar: An example from low density, fire prone ponderosa pine forests. *Forest Ecology and Management*, *208*, 189-209.

Hudak, A. T., Crookston, N. L., Evans, J. S., Falkowski, M. J., Smith, A. M. S., Morgan, P., & Gessler, P. (2006). Regression modeling and mapping of coniferous forest basal area and tree density from discrete-return lidar and multispectral satellite data. *Canadian Journal of Remote Sensing*, *32*, 126-138.

Hyde, P., & Dubayah, R. O. (2005). Mapping forest structure for wildlife habitat analysis using waveform lidar: Validation of montane ecosystems. *Remote Sensing of the Environment, 96*, 427-437.

Hyyppa, J., Hyyppa, H., Inkinen, M., Engdahl, M., Linko, S., & Zhu, Y. H. (2000). Accuracy comparison of various remote sensing data sources in the retrieval of forest stand attributes. *Forest Ecology and Management, 128*, 109–120.

Jenkins, J. C., Chojnacky, D. C., Heath, L. S., & Birdsey, R. A. (2003). National-scale biomass estimators for United States tree species. *Forest Science*, *49*, 12-35.

Jensen, J. R. (2005). *Introductory digital image processing: A remote sensing perspective*. Upper Saddle River, NJ: Prentice–Hall Press.

Jia, G. J., Burke, I. C., Kaufmann, M. R., Goetz, A. F. H., Kindel, B. C., & Pu, Y. (2006). Estimates of forest canopy fuel attributes using hyperspectral data. *Forest Ecology and Management*, *229*, 27-38.

Johnson, E.A. (1992). *Fire and vegetation dynamics*. Cambridge: Cambridge University Press.

Keane, R. E., Garner, J. L., Schmidt, K. M., Long, D. G., Menakis, J. P., & Finney, M. A. (1998). *Development of the input data layers for the FARSITE fire growth model for the Selway-Bitterroot wilderness complex. General Technical Report*

RMRS-GTR-3. Ogden, UT: U.S. Department of Agriculture, Forest Service, Rocky Mountain Research Station 121 pp.

Keane, R. E., Mincemoyer, S. A., Schmidt, K. M., Long, D. G., Garner, J. L. (2000). *Mapping vegetation and fuels for fire management on the Gila National Forest Complex, New Mexico. General Technical Report RMRS-GTR-46.* Ogden, UT: U.S. Department of Agriculture, Forest Service, Rocky Mountain Research Station 126 pp.

Keane, R. E., Reinhardt, E. D., Scott, J., Gray, K., & Reardon, J. (2005). Estimating forest canopy bulk density using six indirect methods. *Canadian Journal of Forestry Research*, *35*, 724-739.

Kilgore, B. M., & Sando, R. W. (1975). Crown fire potential in a sequoia forest after prescribed burning. *Forest Science*, *21*, 83-87.

Korhonen, L., Korhonen, K. T., Rautiainen, M., & Stenberg, P. **(**2006). Estimation of forest canopy cover: a comparison of field measurement techniques. *Silva Fennica*, *40*, 577–588.

Lamont B. B., Korczynskyj D. and Wittkuhn R. (2004). Ecology and ecophysiology of grasstrees. *Australian Journal of Botany, 52,* 561-82.

Lefsky M. A.,Cohen, W. B., Acker, S.A., Spies, T.A., Parker, G.G., & Harding, D. (1999). Lidar remote sensing of biophysical properties and canopy structure of forest of Douglas fir and western hemlock. *Remote Sensing of Environment*, *70*, 339–361.

Lefsky, M. A., Cohen, W. B., Parker G. G., & Harding D. J. (2002). Lidar remote sensing for ecosystem studies. *BioScience*, *52*, 14-25.

Lefsky, M. A., Cohen, W. B., & Spies, T. A. (2001). An evaluation of alternate remote sensing products for forest inventory, monitoring, and mapping of Douglasfir forests in western Oregon. *Canadian Journal of Forest Research*, *31*, 78-87.

Lefsky, M. A., Hudak, A. T., Cohen, W. B., & Acker, S. A. (2005). Patterns of covariance between forest stand and canopy structure in the Pacific Northwest. *Remote Sensing of Environment*, *95*, 517-531.

Li, Y., Andersen, H. E., & McGaughey, R. (2008). A comparison of statistical methods for estimating forest biomass from light detection and ranging data. *Western Journal of Applied Forestry*, *23*, 223−231.

Llinas, J. (2002). Data fusion information. Online at: http://www.infofusion.buffalo.edu/ tm/Dr.linastuff/Da taFusionOverview.ppt#1. (Accessed on February 10, 2010).

Maclean, G. A., & Krabill, W. B. (1986). Gross-merchantable timber volume estimation using an airborne lidar system. *Canadian Journal of Remote Sensing*, *12*, 7– 18.

Maselli, F., Rodolfi, A., Bottai, L., Romanelli, S., & Conese, C. (2000). Classification of Mediterranean vegetation by TM and ancillary data for the evaluation of fire risk. *International Journal of Remote Sensing, 17*, 3303–3313.

Mbow, C., Goita, K., & Benie, G. B. (2004). Spectral indices and fire behavior simulation for fire risk assessment in savanna ecosystems. *Remote Sensing of Environment*, *91*, 1–13.

McAlpine, R. S., & Hobbs M. W. (1994). Predicting the height to live crown base in plantation of four boreal forest species. *International Journal of Wildland Fire, 4*, 103-106.

McCombs, J. W., Roberts, S. D., & Evans, D. L. (2003). Influence of fusing lidar and multispectral imagery on remotely sensed estimates of stand density and mean tree height in a managed loblolly pine plantation, *Forest Science*, *49*, 457–466.

Means, J. E., Acker, S. A., Harding, D. J., Blair, J. B., Lefsky, M. A., & Cohen, W. B. (1999). Use of large-footprint scanning airborne lidar to estimate forest stand characteristics in the western Cascades of Oregon. *Remote Sensing of the Environment*, *67*, 298– 308.

Means, J.E. (2000). Comparison of large-footprint and small-footprint lidar systems: design, capabilities, and uses. *Proceedings of Geospatial Information in Agriculture and Forestry, January 2000* (pp. 185-192). Lake Buena Vista, FL.

Miller, J. D., & Yool, S. R. 2002. Mapping forest post-fire canopy consumption in several overstory types using multi-temporal Landsat TM and ETM data. *Remote Sensing of Environment, 82,* 481-496.

Mitsopoulos, I. D., & Dimitrakopoulos, A. P. (2007). Canopy fuel characteristics and potential crown fire behavior in Aleppo pine (*Pinus halepensis* Mill.) forests. *Forest Science, 64,* 287-299.

Monserud, R. A., & Marshall, J. D. (1999). Allometric crown relations in three northern Idaho conifers. *Canadian Journal Forest Research, 29*, 521–535.

Morsdorf, F., Meier, E., Koetz, B., Itten, K. I., Dobbertin, M., & Allgower, B. (2004).

LIDAR-based geometric reconstruction of boreal type forest stands at single tree level for forest and wildland fire management. *Remote Sensing of Environment, 92,* 353-362.

Mutlu, M., Popescu, S. C., Stripling, C., & Spencer, T. (2008a). Mapping surface fuel models using lidar and multispectral data fusion for fire behavior. *Remote Sensing of Environment, 112*, 274-285.

Mutlu, M., Popescu, S. C., & Zhao, K. (2008b). Sensitivity analysis of fire behavior modeling with lidar-derived surface fuel maps. *Forest Ecology and Management, 256*, 289-294.

Naesset, E. (1997). Estimating timber volume of forest stands using airborne laser scanner data. *Remote Sensing of Environment, 61*, 246-253.

Naesset, E., & Bjerknes, K. O. (2001). Estimating tree heights and number of stems in young forest stands using airborne laser scanner data. *Remote Sensing of Environment, 78,* 328 – 340.

Naesset, E., & Okland, T. (2002). Estimating tree height and tree crown properties using airborne scanning laser in a boreal nature reserve. *Remote Sensing of Environment, 79,* 105-115.

Naesset, E. (2004). Accuracy of forest inventory using airborne laser scanning: evaluating the first Nordic full-scale operational project. *Scandinavian Journal of Forest Research, 19,* 554-557.

Naesset, E., & Gobakken, T. (2005). Estimating forest growth using canopy metrics derived from airborne laser scanner data. *Remote Sensing of Environment, 96*, 453-465.

Næsset, E. & Gobakken, T. (2008). Estimation of above- and below-ground biomass across regions of the boreal forest zone using airborne laser. *Remote Sensing of Environment, 112,* 3079-3090.

National Snow and Ice Data Center website (2010). Satellite ICESat/GLAS waveform data. http://nsidc.org/data/icesat/l aser_op_periods.html. (Accessed on June 21, 2010).

Nelson, R. F., Krabill, W. B., & Maclean, G. A. (1984). Determining forest canopy characteristics using airborne laser data. *Remote Sensing of Environment, 15,* 201– 212.

Nelson, R., Valenti, M. A., Short, A., & Kelley, C. (2003). A multiple resource inventory of Delaware using airborne laser data. *Bioscience, 53*, 981-992.

Nelson, R. F., Ranson, K. J., Sun, G., Kimes, D. S., Kharuk, V., & Montesano, P. (2009). Estimating Siberian timber volume using MODIS and ICESat/GLAS. *Remote Sensing of Environment, 113,* 691-701.

Neuenschwander, A. L., Urban, T. J., Gutierrez, R., & Schutz, B. E. (2008). Characterization of ICESat/GLAS waveforms over terrestrial ecosystems: Implications for vegetation mapping. *Journal of Geophysical Research, 113*, 18-24.

Omi, P. N. (2005). *Forest fires*. Santa Barbara, CA: ABC-CLIO Press.

Pang, Y., Lefsky, M., Sun, G., Miller, M. E., & Li, Z. (2008). Temperate forest height estimation performance using ICESat GLAS data from different observation periods. *Proceedings of the ISPRS ISS VII, June 2008* (pp. 777-782). Beijing, China.

Pereira, J. M. C., Oliveira, T. M. & Paul, J. C. P. (1995). Satellite-based estimation of Mediterranean shrubland structural parameters. *EARSeL Advance Remote Sensing*, *4*, 14–20.

Philip, M. S., (2002). *Measuring trees and forests*. London: CABI Press.

Pollet, J., & Omi, P. N. (2002). Effect of thinning and prescribed burning on crown fire severity in Ponderosa pine forest. *International Journal of Wildland Fire, 11*, 1-10.

Popescu, S. C., Wynne, R. H., & Nelson, R. F. (2002). Estimating plot-level tree heights with lidar: Local filtering with a canopy-height based variable window size. *Computers and Electronics in Agriculture, 37*, 71–95.

Popescu, S. C., Wynne, R. H., & Nelson, R. F. (2003). Measuring individual tree crown diameter with lidar and assessing its influence on estimating forest volume and biomass. *Canadian Journal of Remote Sensing*, *29,* 564-577.

Popescu, S. C., & Wynne, R. H. (2004). Seeing the trees in the forest: Using LIDAR and multispectral data fusion with local filtering and variable window size for estimating tree height. *Photogrammetric Engineering & Remote Sensing, 70*, 589–604.

Popescu, S. C., Wynne, R. H., & Scrivani, J. A. (2004). Fusion of small-footprint lidar and multispectral data to estimate plot-level volume and biomass in deciduous and pine forests in Virginia, U.S.A. *Forest Science*, *50*, 551 -565.

Popescu, S. C. (2007). Estimating biomass of individual pine trees using airborne lidar. *Biomass and Bioenergy, 31,* 646-655.

Popescu, S. C. & Zhao, K. (2008). A voxel-based lidar method for estimating crown base height for deciduous and pine trees. *Remote Sensing of Environment, 112*, 767-781.

Popescu, S. C., Zhao, K., Neuenschwander, A., & Lin, C. (in review). Satellite lidar vs. small footprint airborne lidar: Comparing the accuracy of aboveground biomass estimates and forest structure metrics at footprint level.

Pyne, S. J., Andrews, P. L., & Laven, P. D. (1996). *Introduction to wildland fire*. New York: Wiley & Sons Press.

Ranson, K. J., Lang, R. H., Chauhan, N. S., Cacciola, R. J., Kilic, O., & Guoqing, S. (1997). Mapping of boreal forest biomass from spaceborne synthetic aperture radar. *Journal of Geophysical Research, 102*, 29599-29610.

Ranson, K. J., Sun, G., Kovacs, K., & Kharuk, V. I. (2004). Landcover attributes from ICESat GLAS data in Central Siberia. *Proceedings of the IEEE, 4,* 753-756.

Reinhardt, E. D., Scott, J. H., Gray, K. L., & Keane, R. E. (2006). Estimating canopy fuel characteristics in five conifer stands in the western United States using tree and stand measurements. *Canadian Journal of Forest Research, 36*, 2803–2814.

Research Coordination Network Utilities and Tools (2010). A conversion tool, Montana state university research coordination network, Montana. http://www.rcn.montana.edu/resources/tools/coordinates.aspx (Accessed on June 8, 2010).

Riano, D., Chuvieco, E., Salas, J., Palacios-Orueta, A., & Bastarrika, A. (2002). Generation of fuel type maps from Landsat TM images amd ancillary data in Mediterrannean ecosystem. *Canadian Journal of Forest Research, 32*, 1301-1315.

Riano, D., Meier, E., Allgower, B., Chuvieco, E., & Ustin, S. L. (2003). Modeling airborne laser scanning data for the spatial generation of critical forest parameters in fire behavior modeling. *Remote Sensing of Environment*, *86*, 177-186.

Riano, D., Chuvieco, E., Condis, S., Gonzalez-Matesanz, J., & Ustin, S. L. (2004). Generation of crown bulk density for *Pinus sylvestris* from LIDAR. *Remote Sensing of Environment, 92*, 345 – 352.

Rim, H. J., & Schutz, B. E. (2002), Precision orbit determination (POD), Geoscience Laser Altimeter System (GLAS) algorithm theoretical basis document version 2.2. http://www.csr.utexas.edu/glas/atbd.html. (Accessed on July 19, 2010).

Roccaforte, J. P., Fule, P. Z., & Covington, W. W. (2008). Landscape-scale changes in canopy fuels and potential fire behavior following ponderosa pine restoration treatments. *International Journal of Wildland Fire, 17,* 293-303.

Rothermel, R. C. (1972). *A mathematical model for predicting fire spread in wildland fuels. General Technical Report INT-RP-115*. Ogden, UT: U.S. Department of

Agriculture, Forest Service, Intermountain Forest and Range Experiment Station 8 pp.

Rothermel, R. C. (1983). *How to predict the spread and intensity of forest and range fires. General Technical Report INT-RP-143.* Ogden, UT: U.S. Department of Agriculture, Forest Service, Intermountain Forest and Range Experiment Station 161 pp.

Rollins, M., & Frame, C. (2006). *The LANDFIRE Prototype Project: nationally consistent and locally relevant geospatial data for wildland fire management*. *General Technical Report RMRS-GTR-175.* Fort Collins, CO: U.S. Department of Agriculture, Forest Service, Rocky Mountain Research Station 88 pp.

Russell, W. H., & McBride, J. R. (2003). Landscape scale vegetation-type conversion and fire hazard in the San Francisco bay area open spaces. *Landscape and Urban Planning, 64*, 201–208.

Salas, F. J., & Chuvieco, E., (1995). Aplicacion de imagenes Landsat-TM a la cartografia demodelos de combustible. *Revista de Teledeteccion, 5*, 18–28.

Sando, R. W., & Wick, C. H. (1972). *A method evaluating crown fuels in forest stands. General Technical Report INT-NC-84*. St. Paul, MN: U.S. Department of Agriculture, Forest Service, North Central Forest Experiment Station 72 pp.

Schutz, B. E. (2002), Laser footprint location (geolocation) and surface profiles, Geoscience Laser Altimeter System (GLAS) algorithm theoretical basis document version 3.0, http://www.csr.utexas.edu/glas/pdf/atbd_geoloc_10_02.pdf (Accessed on July 17, 2010).

Scott, J. H., & Reinhardt, E. D. (2001). *Assessing crown fire potential by linking models of surface and crown fire behavior. General Technical Report RMRS-RP-29.* Fort Collins, CO: U.S. Department of Agriculture, Forest Service, Rocky Mountain Research Station 59 pp.

Scott, J. H. (2008). Review and assessment of LANDFIRE canopy fuel mapping procedures. http://www.google.com/search?q=Scott+fuelcalc+and+fmaplus&ie=utf-8&oe=utf-8&aq=t&rls=org.mozilla:en-US:official&client=firefox-a (Accessed on August 9, 2010).

Simard, M., Rivera-Monroy, V. H., Mancera-Pineda, J. E., Castaneda-Moya, E., & Twilley R. R. (2008). A systematic method for 3D mapping of mangrove forests based on Shuttle Radar Topography Mission elevation data, ICEsat/GLAS waveforms and field data: Application to Ciénaga Grande de Santa Marta, Colombia. *Remote Sensing of Environment*, *112*, 2131-2144.

Skowronski, N., Clark, K., Nelson, R., Hom, J., & Patterson, M. (2007). Remotely sensed measurements of forest structure and fuel loads in the Pinelands of New Jersey. *Remote Sensing of Environment, 108*, 123-129.

Smith, L. I. (2002). A tutorial on principal component analysis. http://csnet.otago.ac.nz/cosc453/student_tutorials/principal_components.pdf. (Accessed on January 19, 2010).

Snell, J. A. K., & Brown, J. K. (1980). *Handbook for predicting residue weights of Pacific Northwest conifers. General Technical Report PNW-103*. Portland, OR:

U.S. Department of Agriculture, Forest Service, Pacific Northwest Forest and Range Experiment Station 44pp.

Sprugel, D. G. (1983). Correcting for bias in log-transformed allometric equations. *Journal of Ecology, 64*, 209-210.

Stephens, S. L. (1997). Evaluation of the effects of sivilcultural and fuels treatments on potential fire behavior in Sierra Nevada mixed-conifer forests. *Forest Ecology and Management, 105*, 21-35.

Stratton, R. D. (2004). Assessing the effectiveness of landscape fuel treatments on fire growth and behavior. *Journal of Forestry, 14,* 32-40.

Stukey, J. (2009). Deriving a Framework for Estimating Individual Tree Measurements with lidar for use in the TAMBEETLE Southern Pine Beetle Infestation Growth Model. M.S. thesis, Texas A&M University, College Station, TX.

Sun, G., Ranson, K. J., Kimes, D. S., Blair, J. B., & Kovacs, J. (2008). Forest vertical structure from GLAS: An evaluation using LVIS and SRTM data. *Remote Sensing of Environment, 112*, 107–117.

Taylor, S. W., Baxter, G. J., & Hawkes, B. C. (1998). Modeling the effects of forest succession on fire behavior potential in southeastern British Columbia. *Proceedings of the Fire and Forest Meteorology ADAI Volume II, November 1998* (pp. 2059–2071). Coimbra, Portugal.

Van Wagner, C. E. (1977). Conditions for the start and spread of crown fire. *Canadian Journal Forest Research, 7*, 23-34.

Van Wagner, C. E. (1993). Prediction of crown fire in two stands of jack pine. *Canadian Journal Forest Research, 23*, 442-449.

Varga, T. A., & Asner, G. P. (2008). Hyperspectral and lidar remote sensing of fire fuels in Hawaii Volcanoes National Park. *Ecological Applications, 18*, 613–623.

Westerling, A. L., Gershunov, A., Cayan, D. R., and Barnett, T. P. (2002). Long lead statistical forecasts of area burned in western U.S. wildfires by ecosystem province. *International Journal of Wildland Fire, 11*, 275-286.

Whittaker, R. H., & Woodwell, G. M. (1968). Dimension and production relations of trees and shrubs in the Brookhaven Forest, New York. *Journal of Ecology, 56*, 1-25.

Wulf, R. R. D., Goossens, R. E., Roover, D. P. D., & Borry, F. C. (1990). Extraction of forest stand parameters from panchromatic and multispectral SPOT-1 data. *International Journal of Remote Sensing, 11*, 571–1588.

Xing, Y., Gier, A., Zhang, J., & Wang, L. (2010). An improved method for estimating forest canopy height using ICESat-GLAS full waveform data over sloping terrain: A case study in Changbai Mountains, China. *International Journal of Applied Earth Observation and Geoinformation, 12*, 385-392.

Zwally, H. J., Schutz, B., Abdalati, W., Abshire, J., Bentley, C., Brenner, A., Bufton, J., Dezio, J., Hancock, D., Harding, D., Herring, T., Minster, B., Quinn, K., Palm, S., Spinhirne, J., & Thomas, R. (2002). ICESat's laser measurements of polar ice, atmosphere, ocean, and land. *Journal of Geodynamics, 34*, 405–445.

VITA

Name:	Muge Mutlu
Address:	Spatial Science Lab, Dept. of Ecosystem Science and Management,
	1500 Research Plaza, Office 217, TAMU, College Station, TX 77845
Email Address:	mugekaan@gmail.com
Education:	B.A., Landscape Architecture, Cukurova University, Turkey, 2001
	M.S., Forestry, Texas A&M University, 2006
	Ph.D, Forestry, Texas A&M University, 2010